

R.B.Polder

ELECTRODYNAMICS OF THE AgI/SOLUTION INTERFACE

Proefschrift

ter verkrijging van de graad van
doctor in de landbouwwetenschappen,
op gezag van de rector magnificus,
dr. C.C. Oosterlee,
in het openbaar te verdedigen
op woensdag 19 september 1984
des namiddags om vier uur in de aula
van de Landbouwhogeschool te Wageningen.

BIBLIOTHEEK
DER
LANDBOUWHOGESCHOOL
WAGENINGEN



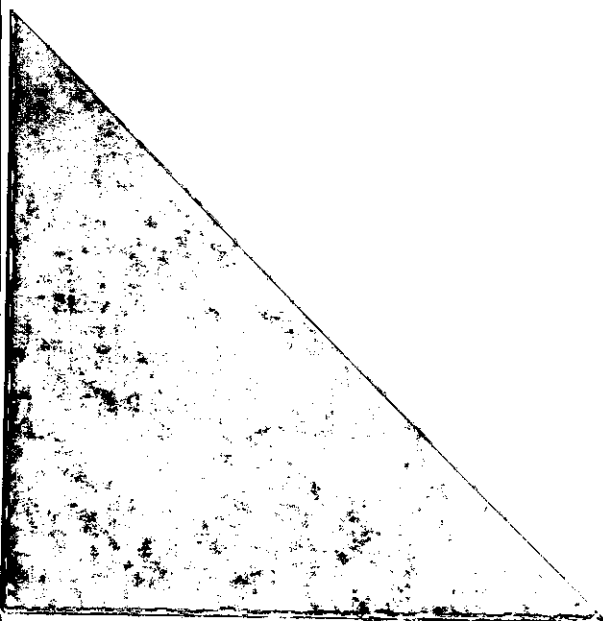
R.B.Polder

ELECTRODYNAMICS OF THE AgI/SOLUTION INTERFACE

Proefschrift

ter verkrijging van de graad van
doctor in de landbouwetenschappen,
op gezag van de rector magnificus,
dr. C.C. Oosterlee,
in het openbaar te verdedigen
op woensdag 19 september 1984
des namiddags om vier uur in de aula
van de Landbouwhogeschool te Wageningen.

BIBLIOTHEEK
DER
LANDBOUWHOGESCHOOL
WAGENINGEN



1. Bratko et al. schatten de nauwkeurigheid van hun geleidingsvermogenmetingen te hoog, gezien de opgegeven nauwkeurigheid van de thermostatisering.

D.Bratko, N.Celija, D.Dolar,
 J.Span, L.Trnkova en K.Vlachy,
 Makromol.Chem., Rapid Commun.,
 4 (1983), 783.

2. Het dalen van de $\omega^{1/2}/Y'$ versus $\omega^{1/2}$ diagrammen bij Kvastek en Horvat moet toegeschreven worden aan de ruwheid van de gebruikte zilverjodide elektroden, en niet aan een adsorptie-impedantie.

K.Kvastek en V.Horvat,
 J.Electroanal.Chem., 147 (1983), 83.
 Dit proefschrift, hoofdstuk III.

3. Uit de afname van de piekhoogte in differentiële puls polarografie (DPP) met toenemende concentratie ligand kan voor metaal-humuszuur oplossingen niet zonder meer gekonkludeerd worden dat het gevormde complex niet labiel is, zoals Ritchie en medewerkers doen voorkomen.

G.S.P.Ritchie, A.M.Posner
 en I.M.Ritchie,
 J. Soil Science, 33 (1982), 671.

4. De formulering van de elektrode-impedantie door Raev et al. is niet in overeenstemming met het door hen gegeven equivalent circuit.

N.D.Raev, I.B.Petkanchin en
 S.P.Stoylov, J.Colloid
 Interface Sci., 96 (1983), 115.

5. Kolawole en Mathieson konkluderen ten onrechte uit veranderingen van de konduktiviteitstoename bij toevoeging van $\text{Cu}(\text{NO}_3)_2$ aan partieel geneutraliseerde PMA-oplossingen dat er sprake is van vier verschillende Cu-PMA complexen; zij houden geen rekening met de binding van K^+ ionen, noch met verdunningseffekten.

E.G.Kolawole en S.M.Mathieson,
 J.Polymer Science, 15 (1977), 2291.

6. De fysische en kolloïdchemie van zilverjodide dispersies zou baat kunnen hebben bij het gebruik van éénkristallen, zoals in de vaste stof chemie gebruikelijk is.

7. Het specifiek oppervlak van zilverjodide is aan golfbewegingen onderhevig.

8. Bij het doorlezen van de landbouwwakbladen krijgt men de indruk dat de wereld bevolkt wordt door dieren en mannen.

9. Het verdient aanbeveling bij inspraakavonden ook achterin de zaal een notulist(e) aantekeningen te laten maken, daar anders wezenlijke informatie verloren kan gaan.

10. Prodeowerk-gevers zijn zelden prodeo-werkgevers.

11. Het belang van het huishoudelijk personeel voor het wetenschappelijk onderzoek wordt onderschat; zonder koffie geen promotie.

12. Het kernwapenbeheersingsbeleid van de NAVO leidt, met instemming van de Nederlandse regering, tot kwantitatieve en kwalitatieve toename van de kernbewapening in Europa.

13. Als werken alles is, zijn teveel mensen niets.

14. De trialsport is de moeite van het proberen waard; de errors komen vanzelf.

Stellingen bij het proefschrift "Electrodynamics of the AgI/solution interface" van R.B.Polder, 19 september 1984.

Opmerkingen vooraf.

Allereerst wil ik Thea, mijn moeder, bedanken voor de soepele wijze waarop ze mij heeft opgevoed en mijn eigen keuzen heeft laten maken, onder haar voortdurende belangstelling. Verder bedank ik Lise, mijn vriendin, voor haar liefdevolle en kameraadschappelijke steun bij dit voor haar weinig begrijpelijke werk, en bij mijn verdere persoonlijke ontwikkeling.

Dan dank ik Bert Bijsterbosch voor de vriendelijke en toch precieze wijze waarmee hij de totstandkoming van dit proefschrift heeft begeleid.

Herman van Leeuwen bedank ik voor zijn grote bijdrage bij de voortgang van dit onderzoek, en zijn vriendschappelijke manier van coachen.

Martien Cohen Stuart heeft me op enkele moeilijke momenten in het werk met zijn ideeën gestimuleerd door te gaan. Jan Scheutjens heeft me vaak geholpen bij kleine en grote problemen met programmeren.

Gert Buurman dank ik hartelijk voor de creatieve wijze waarop hij de tekeningen voor dit proefschrift gemaakt heeft, en voor de gezelligheid en hulp bij onze gezamenlijke hobby. Ronald Wegh heeft veel bijgedragen aan het welslagen van het werk door altijd klaar te staan voor technische vragen, en op het juiste moment de goede adviezen te geven. Henny van Beek heeft steeds snel en nauwkeurig elektroden en andere materialen gemaakt. Willem van Maanen en Ben Spee dank ik voor hun hulpvaardigheid bij het werk en de vele gesprekken erbuiten. Wil van der Made en Yvonne Toussaint wil ik bedanken voor hun medewerking en gezelligheid in de fase van het produceren van dit werk. Yvonne en Olga Hitters dank ik voor het typen van delen van het proefschrift.

Alle niet genoemde huidige en voormalige medewerk(st)ers en studenten/s van de vakgroep Fysische en Kolloïdchemie ben ik dank verschuldigd voor hun hulp en ondersteuning in vele kleine dingen, voor de goede sfeer en voor de belangstelling in mijn persoon.

Buiten de vakgroep gaat mijn dank uit naar Greet Sluyters-Rehbach en Jan Sluyters die op een kritiek moment vriendelijk prikkelende vragen stelden en nuttige suggesties deden. Titus van den Belt bedank ik voor het gebruik van zijn apparatuur voor enkele controlemetingen.

Tot slot wil ik mijn dank uitspreken aan mijn vele vriendinnen en vrienden, in Utrecht, Groningen en Wageningen en elders, die mij tijdens mijn studie, werk en andere activiteiten geholpen hebben, en van wie ik veel geleerd heb.

CONTENTS

	page
Chapter I. Introduction.	1
Chapter II. Materials and methods.	5
Chapter III. The impedance spectrum of the AgI electrode in aqueous solution.	15
Chapter IV. Electrodynamics of the AgI/solution interface. The effect of solution composition and of adsorbed polymer.	35
Chapter V. Electrodynamics of the AgI/solution interface and the meaning for colloid stability.	57
Abstract.	73
Samenvatting.	75
Curriculum vitae.	77

Chapter III is reprinted from the Journal of Electroanalytical Chemistry and Interfacial Electrochemistry 170 (1984), 175-193, by courtesy of Elsevier Science Publishers B.V., and through the kind cooperation of Mr. Leo Konings.

Chapter IV has been submitted for publication in the same Journal.

Chapter I.

INTRODUCTION.

Colloid theory.

The DLVO theory of colloid stability, developed only some forty years ago by Derjaguin and Landau [1] and Verwey and Overbeek [2], has proved to be of great importance, for both theoretical and practical problems. It considers the interaction between charged particles in a lyophobic colloidal solution and it describes colloid stability in terms of the balance between electrostatic repulsion and Van der Waals attraction.

A question that remained unsolved, however, is whether or not the double layers of the particles are at equilibrium with the surrounding solution during the event of a collision. Two extreme cases can be distinguished: (i) during particle encounter the surface charge can adjust itself to the new situation; this is the **constant potential** case; (ii) the particle charge cannot be exchanged with the solution during interaction of the double layers, and the surface potential is changed; this is the **constant charge** case.

Experiments on **suspensions** cannot discriminate between the two limiting cases. Titration measurements ultimately refer to equilibrium conditions, and the definition of the coagulation concentration and its experimental determination are not refined enough. What we need is insight in the electrostatics of the interfaces under study, based on direct information about relaxation phenomena at these interfaces. It is here that dynamic measurements on **electrodes** may contribute to solving the problem.

The model substance AgI.

Model systems have played an important role in the development of colloid science. Natural systems usually suffer from lack of homogeneity and reproducibility, whereas too little is known about their fundamental properties. One of the most widely used model colloids is silver iodide [3]. One can reproducibly make suspensions of this compound, and, provided enough care is taken, well defined electrodes as well. A lot of fundamental knowledge is available on AgI, e.g. electrochemical,

crystallographic and chemical information. The AgI electrode in aqueous solution shows relatively little complications, as contamination by oxygen or organic material can easily be prevented.

Electrodynamics of the AgI/solution interface.

The following chapters will show that we build on a rich tradition of AgI electrode studies. Research-workers at Utrecht (Oomen, Engel and Pieper and De Vooy [4,5,6]), at Wageningen (Peverelli and Van Leeuwen, [7]) and at Zagreb (Kvastek and Horvat, [8]) have investigated the AgI/solution interface since the sixties. Others, like Honig et al., have worked on AgBr [9] or on AgCl, e.g. Ladjouzi [10].

Chapter II describes the preparation of the AgI film electrode, part of the characterization of its surface, the measuring setup and the technique used to obtain the electrodynamic information. It is explained why a new type of silver iodide electrode, the massive silver rod electrode, was introduced.

In chapter III we consider the electrical components of the AgI/-solution interface: the double layer capacitance, the ion transfer resistance and the mass transport impedance. They are discussed in relation to the special features of the material. Based on experimental information an equivalent circuit for the interface and the corresponding impedance equations are presented. Quite some attention is paid to the influence of surface roughness, especially on the mass transport impedance. Taking into account roughness and experimental error, the various methods of impedance analysis are discussed.

Electrodynamics, polymers and colloid stability.

It is well known that polymers may stabilize or destabilize suspensions, e.g., those of silver iodide particles. A notable contribution to the theoretical description of those polymer effects is due to Scheutjens and Fleer [11].

In this work we are concerned with the charge exchange processes during collisions between colloidal particles, and the influence exerted by adsorbed polymers.

In chapter IV we present data on these electrical parameters for electrodes with and without adsorbed polymer (PVA or PVP). Our results are compared with literature data, as obtained from electrode

experiments (capacitance and diffusional parameters), and from titration experiments (capacitances). An attempt is made to explain the dependence of the capacitance and of the diffusion parameter on the potential.

In chapter V we describe the processes contributing to charge adjustment of colloidal particles and their time scales [12,13]. The findings of the previous chapters allow us to revise current notions. For AgI, three different relaxation routes are considered: (i) adjustment of the double diffuse double layer including silver ion conduction inside the solid; (ii) relaxation via migration of Stern ions along the surface of the particle; (iii) diffusion of excess Ag^+ or I^- ions into solution. An electrical equivalent circuit for a particle in interaction is proposed. Finally, the evidence is used to solve the controversy of constant potential vs constant charge.

References.

1. B.V.Derjaguin and L.Landau, Acta Physicochim. URSS, 14, (1941),633.
2. E.J.W.Varwey and J.Th.G.Overbeek, Theory of the Stability of Lyophobic Colloids, Elsevier, Amsterdam 1948.
3. B.H.Bijsterbosch and J.Lyklema, Adv.Colloid Interface Sci., 9, (1978), 147.
4. J.J.C.Oomen, Ph.D. thesis, Utrecht, 1966.
5. D.J.C.Engel, Ph.D. thesis, Utrecht, 1968.
6. J.H.A.Pieper, Ph.D. thesis, Utrecht, 1976;
D.A.De Vooy, Ph.D. thesis, Utrecht, 1976;
J.H.A.Pieper and D.A.de Vooy, J.Electroanal.Chem, 53, (1974), 243.
7. K.J.Peverelli and H.P.van Leeuwen, J.Electroanal.Chem, 99, (1979), 151; 110, (1980), 119, 137.
8. K.Kvastek and V.Horvat, J.Electroanal.Chem, 130, (1981), 67; 147, (1983), 83.
9. E.P.Honig and J.P.M.Huybregts, Proc. 33rd ISE Meeting, Lyon (1982), 825; E.P.Honig and J.H.Th.Hengst, J.Colloid Interface Sci., 31, (1969), 545.
10. M.A.Ladjouzi, Ph.D. thesis, London, 1979.
11. J.M.H.M.Scheutjens and G.J.Fleer, Macromolecules, submitted.
12. J.Lyklema, Pure Appl. Chem., 52, (1980), 1221.
13. J.Lyklema and H.P.van Leeuwen, Adv. Colloid Interface Sci. 16, (1982), 127.

Chapter II.

MATERIALS AND METHODS.

1. Preparation of the electrodes.

a. construction.

In this study we describe a new type of silver iodide electrode. It was introduced because mechanical problems were encountered with the electrodes of the glass tube type that were used in an earlier study [1,2]. Glass tubes frequently broke down during the polishing process, and in other cases the metal film lost contact with the bottom of the glass tube. Electrolytically prepared silver iodide electrodes, often used as reference electrodes, may seem an alternative, but they have a rough surface of which the roughness factor is large but unknown. Ladjouzi reports roughness factors of about 100 for electrolytically grown silver chloride electrodes [3]. In a recent study on rotating silver electrodes Birss and Wright confirm the idea of a very rough surface for electrolytically grown silver iodide [4]. Rough electrodes cause problems in interpreting data, as we will describe in chapter III.

The electrodes used in this study are produced from a massive silver rod embedded in an epoxy resin body. The epoxy resin, Technovit 4071, is very inert and not soluble in water and aqueous solutions. The silver used was Specpure with a purity of 99.999%.

To start the construction of an electrode, a silver rod of 5 mm diameter was machined on one end to a diameter of 3 mm over a length of about 10 mm. The rod was then placed in a tubular holder of approximately 10 mm diameter and the Technovit was poured into the ensuing space. After hardening of the resin and removal of the holder, the encapsulated electrode was machined and provided with a screw hole with thread, as shown in Fig.1. A perspex holder with built-in copper screw and contact wire ensured electrical and mechanical contact with the cell and the measuring circuitry, as displayed in Fig.2.

b. the silver surface.

A clean and smooth silver surface was prepared by grinding flat the encapsulated end of the electrode and polishing it with diamond spray deposited on polishing cloth. In the first stage, diamond particles with

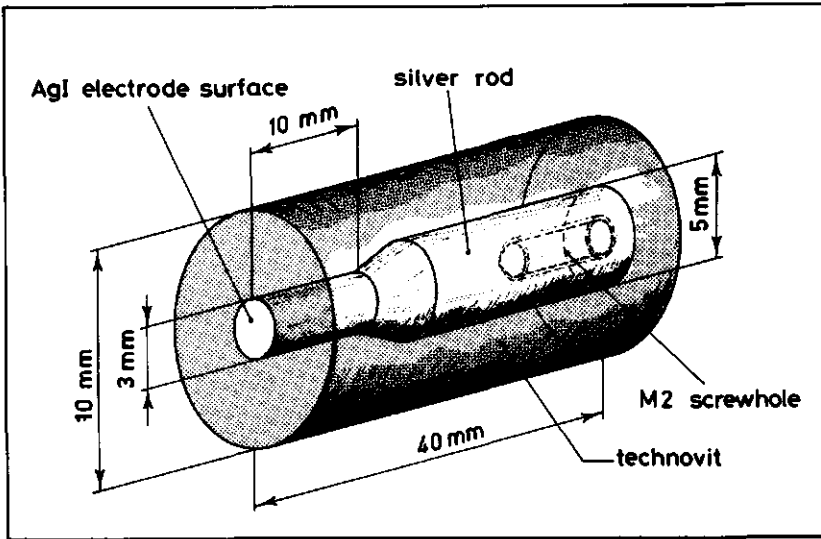


Fig.1 Outline of the construction of the massive silver electrode.

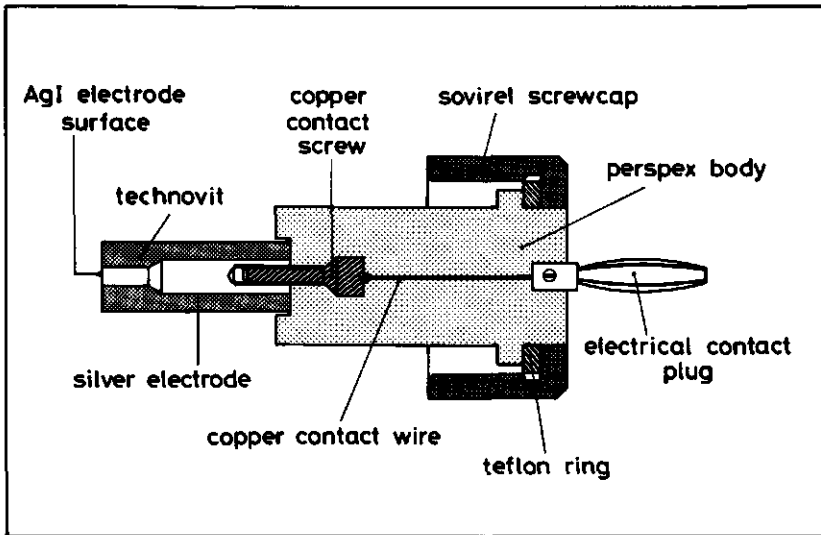


Fig.2. Outline of electrode, electrode holder and electrical contacts.

a size of 6 μm were used, and in the second stage particles of 3 μm . The effect of a third and fourth stage of polishing, with 1 μm and .25 μm particles respectively, has also been investigated. The electrode kinetics, in terms of capacitance and relaxation time, did not differ from electrodes polished down to 3 μm , so in the course of this investigation polishing with particles finer than 3 μm was omitted.

Polishing was frequently interrupted to observe the electrode under a microscope, with a magnification factor of 88 \times , under incident light. The polishing was stopped when the remaining scratches are about 0.3 μm wide and deep, being the dimensions of the sharp edges of 3 μm diamond particles.

Between the polishing and the observation, the electrode was washed with a 1:1 mixture of demineralized water and ethanol, which was also the lubricant on the polishing cloth. The polishing machine rotated at 250 rpm. During polishing the electrode was supported by a perspex holder of 30 mm diameter, with a bore of the same diameter as the electrode. Electrode and electrode holder were pressed on the polishing cloth by light (finger) pressing.

c. the silver iodide film.

After polishing, the electrode was washed thoroughly with the water/ethanol mixture and dried in air. Within half an hour after polishing the silver iodide film was grown on the surface. The film was formed by reaction of the silver substratum with iodine vapour that was developed from a solution of iodine in ethanol (concentration approx. 200 g/l). The electrode was positioned about a centimeter above the solution surface, and was allowed to react for periods ranging from 10 to 30 minutes. The reaction could be followed visually through the bright colouring of the silver surface: within one minute bright red and green colours due to the interference effect in the very thin layer could be observed. In the course of the reaction the colour changed to the mat light brown of the silver iodide. The thickness of the layers thus grown varied between 0.2 and 1.0 μm , depending on the reaction time. Layer thicknesses were measured by stripping the silver iodide from the electrode with a constant current, as previously described by Peverelli et al. [2]. The potential was monitored to detect the time needed for complete stripping. During the electrolysis the potential was about -325 mV vs SCE, due to the reaction $\text{AgI} + e = \text{Ag} + \text{I}^-$. When the stripping of

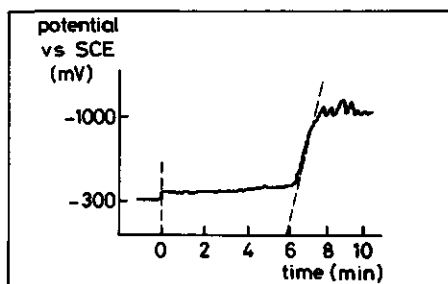


Fig.3. Potential of the AgI/solution electrode vs SCE as a function of time during the stripping process. Electrolyte 0.1 M KI.

the AgI was completed, the potential rose steeply to about -1000 mV vs SCE, due to the reaction $\text{H}_2\text{O} + e = \frac{1}{2} \text{H}_2 \uparrow + \text{OH}^-$. A typical potential time curve is shown in Fig.3. The electrolyte used was 0.1 M KI. The amount of silver iodide stripped is equal to the product of time t and current I , typically in the order of a few minutes and 30 μA . With the known geometrical area A of the film and the known specific density ρ the thickness d can be estimated:

$$d = I t / F \rho A. \quad (1)$$

There is little porosity and the irregularities on the surface have small dimensions as compared to the total thickness. We refer to the Scanning Electron Micrographs and the discussion in the experimental section of Chapter III.

d. the ageing of the silver iodide film.

In order to obtain a sufficiently crystalline AgI film with stable properties, the electrodes were aged. This ageing was performed in a solution of 10^{-3} M KNO_3 and 10^{-4} M KI at a temperature of 80 °C for 60 to 80 hours. This procedure, which is known to yield AgI with reproducible properties as shown in various colloid chemical investigations [5], was also used by Peverelli and Van Leeuwen [2].

Freshly prepared electrodes showed a larger capacitance than aged ones. We conclude that the surface roughness is reduced by ageing. This is probably due to Ostwald ripening (growth of the larger irregularities at the expense of the smaller ones, thus overall reducing the real surface area), coupled with an increase in crystallinity.

2. Other materials.

Throughout this study the supporting electrolyte was 0.1 M KNO_3 . This solution was made up with what is called AgI-water, prepared from demineralized water by slowly passing it through a column of precipitated AgI. In this way any traces of surface active molecules, that tend to adsorb onto AgI, are removed. KNO_3 was dissolved in AgI-water and stirred overnight at 80 °C in the dark with some silver iodide precipitate to remove all surface active material from the salt solution. After filtering off the precipitate, the KNO_3 solution was diluted to 0.1 molar. The nitrogen bubbling through the cell between experiments was purified by successively passing it through concentrated H_2SO_4 - and KOH-solutions and by leading it over a copper catalyst.

The ethyleneglycol used was reagent grade quality and was not further purified. The poly(vinylpyrrolidone) (PVP) used was a BASF commercial product, having a molecular weight of approx. 900,000. The poly(vinylalcohol) (PVA) used was from a sample prepared by Scholtens (batch B4) [6]. It had a molecular weight of about 90,000, and contained 20% acetate groups, in a blocky distribution.

3. The relaxation measurement.

a. the cell.

A broad outline of the cell has been described elsewhere [7]. We will give some more details here. The cell consists of a covered double-walled glass vessel of approx. 250 ml volume, containing the solution, two identical silver iodide electrodes, a gas inlet and a salt bridge for contact with a reference electrode. It is shown in Fig.4. In the relaxation experiments the two AgI electrodes are employed; for the potentiometric determination of the Ag^+ or I^- activity in the solution one of the AgI electrodes and a saturated calomel reference electrode are employed. The salt bridge is a vertical glass tube with a glass frit at the bottom. The bridge is filled with 0.1 M KNO_3 and leakage is as small as 0.1 ml per day. The electric resistance of the bridge is a few hundred kilo-ohms and its approximate value is exploited as a check for good functioning. To avoid interference of e.g. diffusion potentials, the potentiometric determination of $[\text{Ag}^+]$ or $[\text{I}^-]$ was calibrated with solutions of known concentrations. Between subsequent relaxation measurements the solution is stirred with a magnetic stirrer. The cell

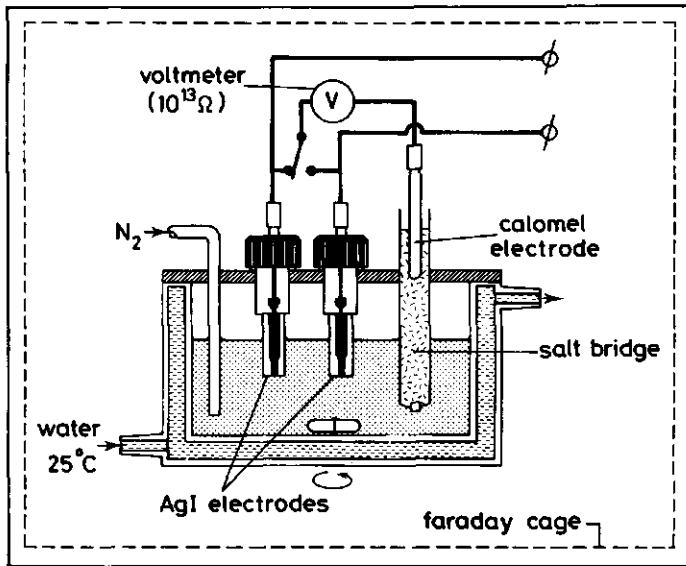


Fig.4. The cell.

is placed in a Faraday cage. Given the high concentration of inert electrolyte, the position of the electrodes with respect to each other is unimportant.

b. the coulostatic impulse method.

The technique used to study the dynamics of the silver iodide/solution interface is the coulostatic impulse method. This method is chosen for its simplicity of instrumentation, its relative insensitivity to cell resistance and its capability of detecting rather fast processes.

The coulostatic impulse method has been introduced independently by Barker [8], Reinmuth [9] and Delahay [10]; it was further developed, e.g. in the field of electrode kinetics, by Kooijman and Sluyters [11] and Weir and Enke [12]. Recently Van Leeuwen has reviewed the method and has given full account of its special properties [13,14].

The coulostatic method is based on a charge injection to the electrode under study. The time scale is chosen so short that only the electrical double layer capacitance is charged; the initial departure from the equilibrium potential is simply determined by:

$$E - E_{eq} = \eta = \Delta q / C \quad (2)$$

where E is the actual potential, E_{eq} the equilibrium potential, η the overvoltage, Δq the impulse charge density and C the double layer capacitance. After cessation of the pulse, the overvoltage is observed at open circuit. This decay represents the relaxation of the double layer capacitance via the faradaic (ion transfer) impedance. The decay signal is recorded, and can be analyzed either directly in the overvoltage-time domain, or in the impedance-frequency domain.

Principally the setup consists of a high power pulse generator in series with a resistance, and a fast voltage recording system [13], as schematically pictured in Fig.5.

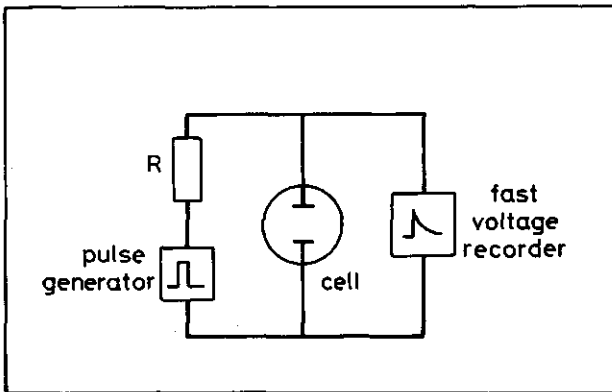


Fig.5. The principle of the coulostatic setup.

For a pulse to be really coulostatic, it must be short with respect to the relaxation times of the faradaic processes at the interface. The coulostatic nature of the pulse can be checked by varying the load resistance R and/or the pulse duration (with constant total charge), which should have no effect on the decay curve. In our experiments both requirements were fulfilled.

c. the instrumental setup.

The instrumental setup is displayed in Fig.6. The coulostatic charge pulse in our experiments originates from a Hewlett-Packard high power pulse generator type 214A. Any overshoot from the charging pulse in the decay signal is cancelled by the circuitry: the output signal is proportional to the potential difference between the cell and a compensating resistance R_c . Before the experiment R_c is given the approximate value of the total cell resistance R_Ω (which includes solution resistance).

The transient is recorded by a Datalab Transient Recorder, type

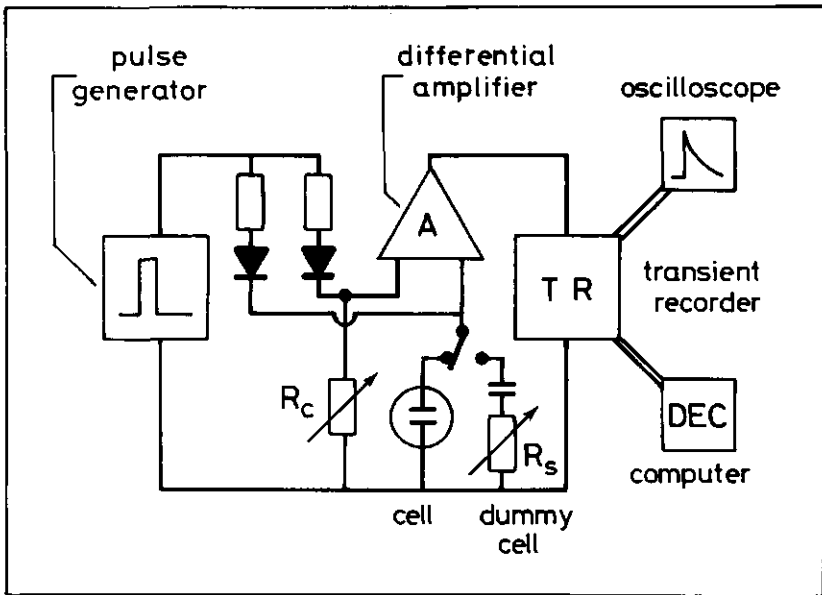


Fig.6. The instrumental setup.

DL905, and transmitted through a fast data line to a DEC-10 computer for processing. The signal is monitored by an oscilloscope for visual observation. The timescale of the complete decay of the transients ranges from 0.1 to 1.0 second. The magnitude of the charge pulse is measured by monitoring the potential rise over a known capacitance in a dummy cell as it results from a test pulse. The series resistance R_s of the dummy cell is identical to the series resistance of the cell, R_Ω . This value is known with sufficient accuracy from the value of the compensating resistance R_c . The amount of charge injected is such that the amplitude of the disequilibrium is always below 25 mV, which seems to be the limit for the region of linearity of the potential-current relation. For more details the reader is referred to [13]. The evaluation of the kinetic parameters will be described in chapter III.

d. the transformation of the signal.

The signal from the relaxation apparatus described in the previous sections is essentially a voltage-time signal. In order to facilitate the analysis, the signal is transformed into an impedance- and/or admittance-frequency spectrum. The transformation procedure used in this study is the same as described by Peverelli and Van Leeuwen [7]. In principle it is possible to transform a $V(t)$ signal made up of n data

points (V_1 at time t_1 to V_n at time t_n) to a complex impedance (or admittance) spectrum with angular frequencies ranging from $1/t_n$ to $1/t_1$. The impedance is given by $Z(\omega) = Z' - j Z''$, the admittance by $Y(\omega) = Y' + j Y''$, where Z' and Y' are the real and Z'' and Y'' the imaginary components and $j = \sqrt{-1}$. And, of course, $Z(\omega) = 1 / Y(\omega)$.

The impedance is obtained by [13]:

$$Z(\omega) = \bar{V}(\omega) / \bar{I}(\omega) \quad (3),$$

where $\bar{V}(\omega)$ and $\bar{I}(\omega)$ are the Laplace transforms of overvoltage and current respectively. The transform of the current i is very simple for the coulostatic case [13]:

$$\bar{I}(\omega) = \int i(t) \exp(-j\omega t) dt = \int q \delta(t) \exp(-j\omega t) dt = q \quad (4)$$

with $\delta(t)$ being the Dirac delta function.

The transform of $V(t)$ is found by describing the overvoltage by a linear combination of trial functions with known transforms:

$$V(t) = \sum c_i f_i(t) \quad (5)$$

The coefficients c_i are found by a computer fitting procedure using least squares analysis; the time constants of the trial functions $f_i(t)$ are chosen to be evenly spread over the timescale of the $V(t)$ signal. The program uses three error functions and three exponential functions as trial functions. The transform of the overvoltage follows from the linear combination of the transforms of the trial functions:

$$\bar{V}(\omega) = \sum c_i \bar{F}_i(\omega) \quad (6)$$

The correctness of the transformation procedure was verified by using different trial functions. The correctness of the whole method of obtaining impedance spectra was checked by the analysis of dummy circuits with resistances and capacitances of known magnitudes and by measuring one or two sets of data with an A.C. bridge. Considering the level of experimental error, the results were satisfactory for these comparisons.

4. References.

1. K.J.Peverelli, Ph.D. thesis, Wageningen, 1979.
2. K.J.Peverelli and H.P.van Leeuwen, *J.Electroanal.Chem.*, **99** (1979), 151.
3. M.A.Ladjouzi, Ph.D. thesis, London, 1979.
4. V.Birss and G.A.Wright, *Electrochim.Acta*, **27** (1982), 1439.
5. B.H.Bijsterbosch and J.Lyklema, *Advances Colloid Interface Sci.*, **9** (1978), 147.
6. B.J.R.Scholten, Ph.D. thesis, Wageningen, 1977.
7. K.J.Peverelli and H.P.van Leeuwen, *J.Electroanal.Chem.*, **110** (1980), 119.
8. G.C.Barker, in *Trans Symp. Electrode Proc.*, Philadelphia, 1959 (E.Yeager ed.), Wiley, New York, 1961.
9. W.H.Reinmuth, *Anal.Chem.* **34** (1962), 1272.
10. P.Delahay, *J.Phys.Chem.*, **66** (1962), 2204; *Anal.Chem.* **34** (1962), 1267.
11. D.J.Kooijman and J.H.Sluyters, *Electrochim.Acta*, **12** (1967), 1579.
12. W.D.Weir and G.C.Enke, *J.Phys.Chem.*, **71** (1967), 280.
13. H.P.van Leeuwen in *Electroanalytical Chemistry*, A.J.Bard (ed.), Vol 12., Marcel Dekker, New York, 1982, p.159.
14. H.P.van Leeuwen, *Electrochim.Acta*, **23** (1978), 207.

J. Electroanal. Chem., 170 (1984) 175-193
Elsevier Sequoia S.A., Lausanne - Printed in The Netherlands

Chapter III.

THE IMPEDANCE SPECTRUM OF THE AgI ELECTRODE IN AQUEOUS SOLUTION

ROB B. POLDER, BERT H. BLIJSTERBOSCH and HERMAN P. VAN LEEUWEN *

*Laboratory for Physical and Colloid Chemistry, Wageningen Agricultural University, De Dreijen 6,
6703 BC Wageningen (The Netherlands)*

(Received 16th December 1983; in revised form 15th February 1984)

ABSTRACT

The dynamic properties of the double layer at the AgI/solution interface are discussed in terms of the relation between Ag^+ interstitials in the AgI phase and the composition of the aqueous solution. Owing to the relatively short relaxation time of the space charge in AgI, the capacitance of the double layer may be regarded as a pure capacitance in the frequency range covered by the impedance measurements. Other possible components of the interfacial impedance are an ion-transfer resistance and a Warburg impedance for transport of Ag^+ (or I^-) in solution. The latter may exhibit a complicated frequency dependence due to the roughness of the AgI surface. It is explained how in the past this complication has led to incorrect interpretation of the impedance spectrum. Experimental impedance data have been obtained by the coulostatic impulse technique. Different ways of impedance spectrum analysis are discussed, taking into account the effect of surface roughness on the mass transport impedance. It is pointed out that the analysis of the real and imaginary components of the admittance gives the best results.

From the present analysis it is concluded that interfacial ion transfer is fast, and that relaxation processes are fully described by the double-layer capacitance and diffusional mass transport in solution.

INTRODUCTION

Electrode impedance analysis, as developed by, for example, Sluyters-Rehbach and Sluyters [1], has been applied to the AgI/solution interface in a number of studies [2-8]. In part, these studies were aimed at elucidating the static properties of the interfacial double layer, to allow independent verification of the surface charge/potential relationship as obtained by potentiometric titrations of suspensions [9].

Another objective has been the quantitative characterization of the interfacial ion transfer kinetics [6,7], which is required for describing double-layer relaxation processes in an AgI sol [10,11]. These studies cover a wide frequency range, including low frequencies where faradaic processes play a role.

The AgI/solution system has some special features. First of all, the AgI surface

* To whom correspondence should be addressed.

has a certain degree of roughness, even in the case of carefully prepared film electrodes [5]. Secondly, the conductance of the AgI is such that an interfacial charge will be smeared out: the space charge layer [12]. The magnitude of this space charge is related to the activities of the electroactive species Ag^+ and I^- in the solution. Thirdly, it is well known that the only mobile charge carriers in the solid AgI phase are the interstitial Ag^+ ions [13]. All of these aspects will be taken into account in formulation of the equations and analysis of the impedance.

We feel the need to reconsider analysis methods, because those presented up to now show unsatisfactory features. Firstly, the method based on separation of the faradaic impedance suffers from methodical contradictions: the two components are not parallel in the graph, the two curves are not straight lines and the imaginary curve does not go through the origin [6]. Secondly, a more involved admittance analysis [8] is based on a disputable circuit description, i.e. it would hold for a redox system with adsorption of the electroinactive species. Furthermore, it contains an unrealistic Warburg impedance for mass transport in the solid AgI phase, and the treatment of surface roughness is inconsistent with the experimental data.

In this article we will discuss several methods of analysis of the AgI/solution interfacial impedance, illustrated by some data obtained by the coulostatic impulse method [14]. More extensive results, including experiments on electrodes with adsorbed small organic molecules and polymers, will be published in a forthcoming article [15].

EXPERIMENTAL

The AgI electrodes consisted of a flat, thin layer (thickness between 300 and 1000 nm) of AgI, grown by reaction with iodine vapour (from an iodine solution in ethanol), on a polished massive silver substratum. Scanning electron micrographs showed that the AgI surface contained irregularities of the order of 300 nm. This means that in the frequency range used ($5 \dots 2000 \text{ rad s}^{-1}$) diffusion towards the electrode surface can be considered diffusion to/from a plane. The electron micrograph is shown in Fig. 1. In the text these electrodes are referred to as "flat" electrodes. Inclusion of ethanol was ruled out since Electron Backscattering experiments showed no sign of oxygen.

Electrodes having a deliberately rough surface were prepared by electrolytically growing the AgI film on polished massive silver. The growing conditions were: current density $4 \times 10^{-4} \text{ A cm}^{-2}$, electrolyte 0.1 M KI. The calculated average thickness of the AgI film was 3 μm . After electrolysis the electrodes were aged for 72 h at 80°C at pH 4. A micrograph of this type of electrode is shown in Fig. 2. It can be seen that considerable roughness is present, with an average grain size of ca. 3 μm . We will refer to these electrodes as "rough". As the grain size is in the order of, or even larger than, the average film thickness, the question arises whether the Ag substratum is completely covered with AgI. Electron Backscattering experiments showed that the whole surface was covered with Ag and I in equal amounts,

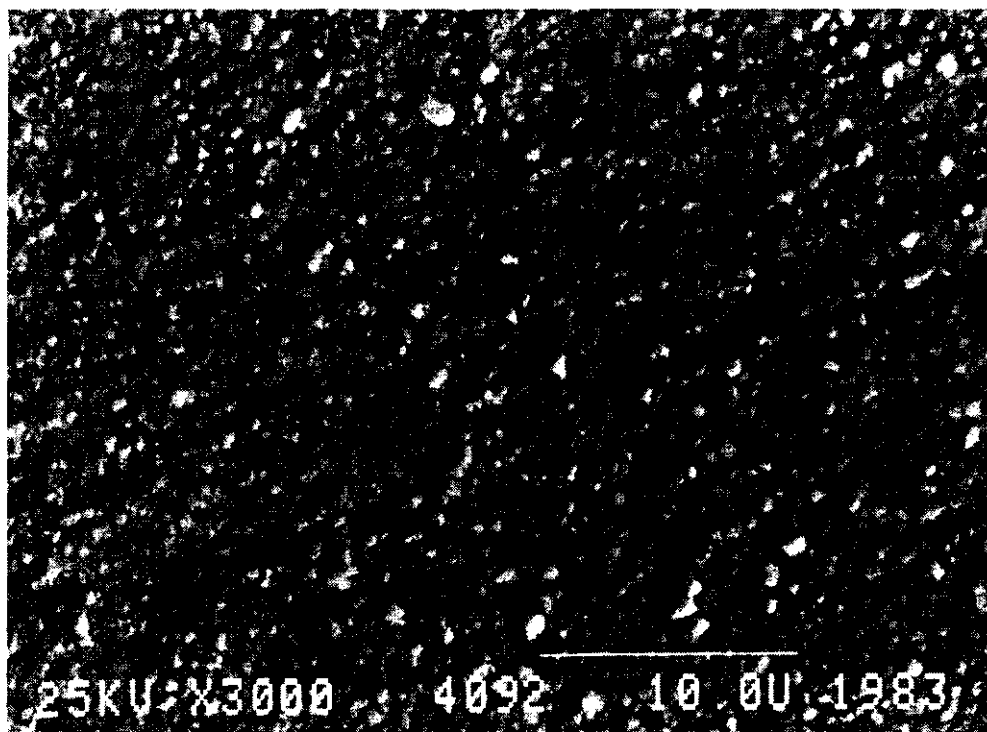


Fig. 1. Scanning electron micrograph of an AgI electrode, grown from iodine vapour ("flat electrode"). The bar indicates 10 μm .

including the regions between the coarsest grains. This applied to both "flat" and "rough" electrodes.

The equilibrium potential was adjusted by adding small amounts of either KI or AgNO_3 solutions.

The relaxation technique used was the coulostatic impulse method. It has the advantage over bridge impedance measurements of the absence of a contribution from the series resistance ensuing from the solution or the solid state. It involves a short ($< 1 \mu\text{s}$) charging impulse (applied to the two identical electrodes) and subsequent measurement of the resulting potential/time transient. The data were analysed after transformation of the transient into an impedance-frequency spectrum. The experimental setup was essentially the same as that described earlier [6]. It has been shown before [4,6] that under the given conditions the Ag/AgI interface does not contribute to the overall electrode impedance. For more detailed information on materials and methods the reader is referred to a forthcoming publication [16].

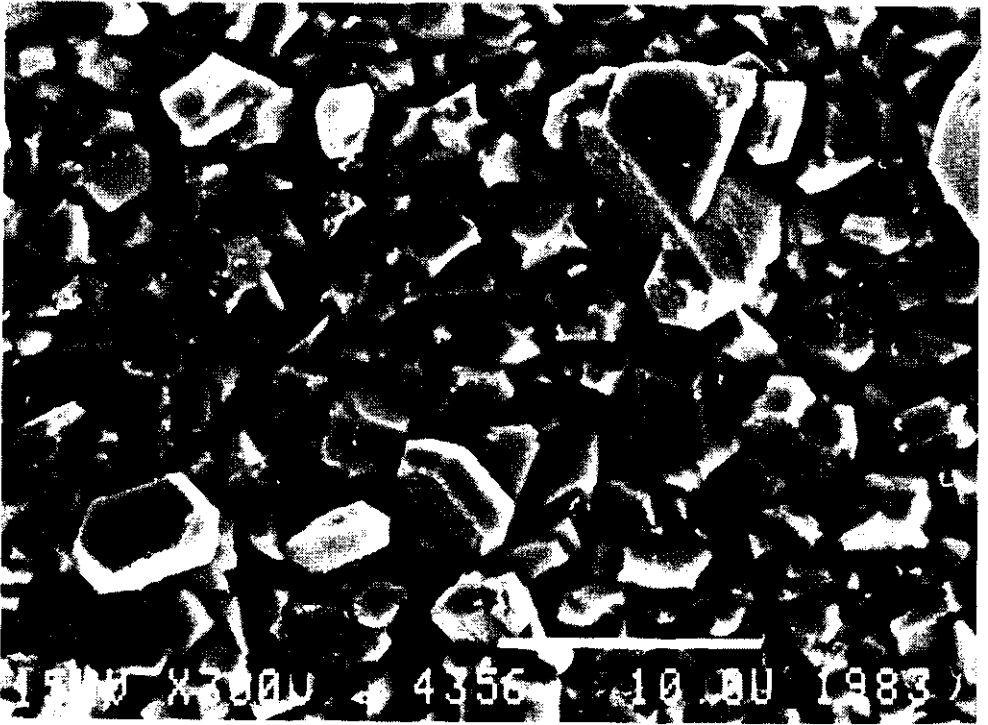


Fig. 2. Scanning electron micrograph of an electrolytically grown AgI electrode ("rough electrode"). The bar indicates 10 μm .

ELECTRODYNAMICS OF THE AgI/SOLUTION INTERFACE

Between the two homogeneous phases an interfacial region exists, where the properties differ from those in the bulk phases. In the case under consideration, the solid phase consists of silver and iodide ions in a crystal packing. At room temperature the pure crystal has a Frenkel defect structure, i.e. equilibrium exists between mobile interstitial silver ions (Ag_i^+) and an equivalent amount of silver ion vacancies ($[\text{V}_{\text{Ag}}^-]$),



where the left-hand side denotes an Ag^+ ion at a lattice site. Iodide ions in the solid are immobile.

When the solid is in equilibrium with an aqueous solution, the AgI crystal has acquired a net charge, the sign and magnitude of which depend on the activities of the constituent Ag^+ and I^- ions in solution. Honig and co-workers [12] have shown that this charge is present in the AgI phase as an excess of Ag_i^+ or V_{Ag}^- , in a space

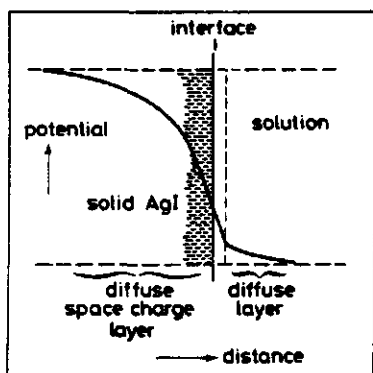


Fig. 3. The potential profile across the AgI/solution interface. The charge-free layer adjacent to the interface is the Stern layer.

charge region adjacent to the interface. The thickness of this part of the electrical double layer was estimated to be about 50 nm [11].

Thus at the AgI/aqueous solution interface a situation exists that is sometimes called a double diffuse double layer (see Fig. 3). If, for example, the activity of Ag^+ in solution is increased, the excess of Ag_i^+ in the solid increases, according to the exchange equilibrium



Any change of the Ag^+ (or I^-) activity in solution is coupled to a change of the ratio $\text{Ag}_i^+ / \text{V}_{\text{Ag}^+}^-$; that is, it affects the net charge on the AgI. The validity of this picture has been confirmed by experiments with doped silver halide crystals [12]. Apart from this variable space charge inside the AgI solid, there may also be a permanent charge in the surface layer of the AgI. This charge would be connected to the solid-state properties of the outermost layer of the AgI phase, which would differ from the bulk [12]. This charge is independent of the Ag^+ and I^- activities in solution [17], and hence is of no concern in impedance studies where only changes in charge distribution are effective.

It is worthwhile noting that the AgI/solution interface is a non-polarizable one, just like the metal/metal ion electrode interface. This means that any change of the Ag^+ activity in solution leads to a corresponding change in the net charge on the AgI, and a related change in the (reversible) interfacial potential difference. These three parameters represent only *one* real variable quantity, in contrast to the more general situation of a redox couple $\text{Ox} + n e^- \rightleftharpoons \text{Red}$, with Ox and/or Red being surface-active. There one has *two* independent variables for the reversible case [18].

The situation at the AgI/solution interface is dynamic, since there is a continuous

exchange of silver and iodide ions between the solid and the solution. In equilibrium the net ionic current is zero; if the electrode is forced away from equilibrium, as in the relaxation experiment, there will be a net flow of ions in one direction in order to restore equilibrium. Combining eqns. (1) and (2) gives:



This is the process of net interfacial charge transfer with silver ions, and



is the process of exchange with iodide ions in solution. The resemblance to the metal/metal ion electrode interface is obvious. Equation (3) is analogous to $\text{Me} \rightleftharpoons \text{Me}^+ + e^-$, with the silver vacancy playing the role of the electron in the AgI case.

EQUIVALENT CIRCUIT REPRESENTATION

Components of the impedance

The AgI/solution interface, as described in the previous section can be represented electrically by:

(a) A double-layer capacitance, C , depicting the accumulation of charge in the double layer. This includes the space charge layer in the solid and the diffuse double layer extending into the solution (where interstitial silver ions and inert electrolyte ions are the main charged species, respectively). We may consider the complete double-layer capacitance as a pure capacitance because the processes of charging are relatively fast compared to the timescale covered by our experiments. Charging of the space charge layer is fast as a result of the relatively high conductivity and the low permittivity of AgI [5]. The time constant for this dielectric relaxation is ca. 10^{-8} s. Charging of the diffuse double layer is even faster: ca. 10^{-9} s for an electrolyte concentration of ca. 0.1 M.

(b) A charge-transfer resistance, θ , reflecting the activation energy for transfer of silver (or iodide) ions through the interface.

(c) A diffusional impedance, Z_w , describing the transport of silver or iodide ions in the solution. Due to the high excess of indifferent electrolyte in the solution, the transport numbers of silver and iodide are effectively zero, so these ions move only as a result of a concentration gradient. For a flat surface this process is represented by the well-known Warburg impedance [19]:

$$Z_w = (1 - j)\sigma\omega^{-1/2} \quad (5)$$

where $j = (-1)^{1/2}$, ω is the angular frequency, and σ is given by:

$$\sigma_i = (2D_i)^{-1/2}(c_i)^{-1}RT/F^2 \quad (6)$$

where D_i and c_i are the diffusion coefficient and solution concentration of ion i , respectively, and R , T and F have their usual meaning. In the solid AgI phase the

situation is quite different: the only mobile species is $\text{Ag}_i^+(t_{\text{Ag}_i^+} \sim 1)$ [13], so the electrical migration process is dominant and consequently there will be no Warburg behaviour.

In the case of bridge impedance measurements, a series resistance is necessary to account for the bulk resistance of the solution and/or solid phase. When the coulostatic method is applied, there is no net current flowing through the cell during the actual measurement, so there is no need to consider the additional series resistance [14].

The complete equivalent circuit

A double-layer capacitance, a charge-transfer resistance and a diffusion impedance represent the electrical response of the AgI/solution interface. It has been pointed out well enough [1,18,20] that for the reversible metal ion/metal electrode the coupling of faradaic processes and double-layer charging results in impedance equations corresponding to a Randles type of circuit. In this circuit the adsorption term is included in the capacitive component in the form of a term $d\Gamma/dE$. In the previous section we explained that the AgI/solution interface obeys the same principles, and this means a parallel configuration of the capacitive branch (incorporating the adsorption) and an ion-transfer ("faradaic") branch. The circuit is illustrated in Fig. 4. Note that for an AgI *particle* in a suspension the interface is isolated, and this means that the two branches are essentially in series. Contrary to the case of an *electrode*, there is no external circuit and the double layer can only be charged by ion transfer through the interface.

Pieper and De Vooy's [4] and Peverelli and Van Leeuwen [6] have shown that the Randles circuit is a useful tool to elucidate the interfacial behaviour of AgI in aqueous solution. Others have added components or have modified the circuit. Ladjouzi, for example, has added a surface diffusion impedance in his analysis of AgCl/solution interfaces [21]. Kvastek and Horvat [8] have seen reason to modify the impedance to account for an adsorption step, using Timmer's [18] admittance

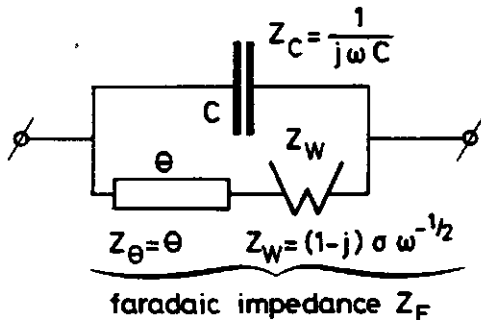


Fig. 4. The Randles equivalent circuit for an electrode, with its different components and their impedances.

equations for the case of adsorption of electroinactive species. However, the adsorption of Ag^+ and I^- ions is already accounted for by the capacitance, as pointed out above.

Impedance and admittance equations

The impedance and admittance of the Randles circuit in terms of the three constituents can be formulated as [1]:

$$Z_{\text{Randles}} = \frac{(\theta + \sigma\omega^{-1/2}) - j[\omega C(\theta + \sigma\omega^{-1/2})^2 + \sigma\omega^{-1/2}(1 + \sigma\omega^{1/2}C)]}{(1 + \sigma\omega^{1/2}C)^2 + \omega^2 C^2(\theta + \sigma\omega^{-1/2})^2} \quad (7)$$

$$Y_{\text{Randles}} = \frac{(\theta + \sigma\omega^{-1/2}) - j\sigma\omega^{-1/2}}{(\theta + \sigma\omega^{-1/2})^2 + \sigma^2\omega^{-1}} - j\omega C \quad (8)$$

where $j = (-1)^{1/2}$, and ω is the angular frequency in rad s^{-1} . Depending on the conditions, either charge transfer or mass transport may be dominant in the faradaic branch. As we will show, the latter case is met in our experiments, and then Z and Y reduce to:

$$Z_{\theta=0} = \frac{\sigma\omega^{-1/2} - j\sigma(\omega^{-1/2} + 2\sigma C)}{(1 + \sigma\omega^{1/2}C)^2 + \omega C^2\sigma^2} \quad (9)$$

$$Y_{\theta=0} = (1 - j)\omega^{1/2}/2\sigma - j\omega C \quad (10)$$

Figure 5 illustrates the $Z'-Z''$ complex plane representation (open circles). In the following we will use Z' and Y' for the real, Z'' and Y'' for the imaginary parts of impedance and admittance.

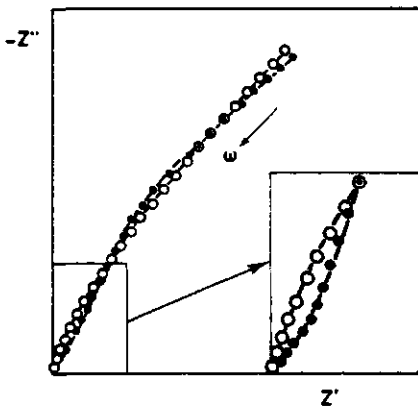


Fig. 5. Impedance plane plot for the case where diffusion is dominant ($\theta \rightarrow 0$). (O) Flat electrode (= Randles, calculated); (●) rough electrode, measured, $f_R = 5$, $l_R = 3 \mu\text{m}$.

Surface roughness

The diffusion impedance used in the Randles circuit needs further attention: *the circuit and equations given apply only to flat electrodes*. We will illustrate the problems caused by surface roughness here, and describe some consequences in more detail in following sections.

The complications for the impedance caused by the roughness of the electrode surface were recognized as early as about 30 years ago, when Lorenz [22] reported frequency-dependent diffusion impedances for polycrystalline (rough) cadmium electrodes. Some 10 years later, De Levie [23,24] discussed the same phenomenon and warned against the interpretation in terms of adsorption before the possibility of surface roughness had been ruled out [25]. Vetter described a similar frequency-dependent diffusion parameter for the case of small active centres on a partly covered metal electrode [26]. The Warburg diffusion impedance is defined for semi-infinite linear diffusion to or from a flat surface and the Warburg coefficient σ , as given by eqn. (6), corresponds to the flat surface area A_{geom} . If the electrode surface is rough, this only holds for low frequencies, when the diffusion layer thickness δ , estimated by $(\pi D_i/\omega)^{1/2}$, is large compared to the average size l_R of the irregularities. This holds for

$$\omega \ll \pi D_i/l_R^2 \quad (11)$$

We denote the Warburg coefficient for low frequencies as σ_{LF} . For relatively high frequencies (short time for diffusion) the diffusion layer thickness is smaller than the size of the irregularities:

$$\omega \gg \pi D_i/l_R^2 \quad (12)$$

and the layer follows the whole, rough, microscopic surface, so that σ_{HF} corresponds to the microscopic surface area. The relation between the extreme cases is

$$\sigma_{\text{LF}} = f_R \sigma_{\text{HF}} \quad (13)$$

with the roughness factor defined as

$$f_R = A_{\text{micr}}/A_{\text{geom}} \quad (14)$$

Three diffusion layer thicknesses and a schematic diagram of the surface roughness are given in Fig. 6. In between the low and high frequency ranges the order of magnitude of the diffusion layer thickness is comparable to that of the surface irregularities. Calculations for this transition region are difficult to do because the flux distribution is no longer homogeneous. The simple Warburg impedance is no longer valid, and so the Randles circuit can no longer be applied [25]. For an apparent Warburg coefficient, σ_{app} , we expect, however, a smooth transition from the high frequency to the low frequency situation.

It may be concluded that the applicability of the simple Randles circuit for the analysis of the AgI/solution interfacial impedance depends on proper matching of the frequency range and surface irregularities: the smaller l_R , the higher the

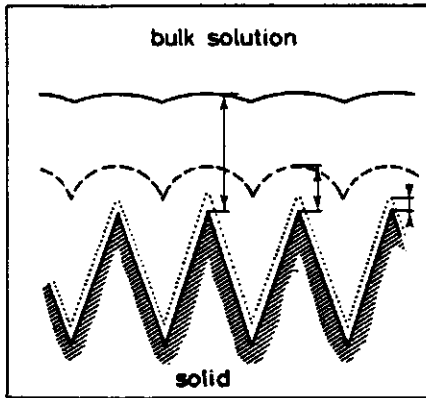


Fig. 6. Diffusion layer thickness and surface roughness; the diffusion layer thickness (\leftrightarrow) is indicated for high (.....), middle (---) and low (—) frequencies.

frequencies that can be analysed. Our experimental results support this conclusion as we will show in the following sections.

ANALYSIS BASED ON THE RANDLES CIRCUIT

Impedance and admittance spectra for the AgI/solution electrode can be analysed in various ways based on the Randles equivalent circuit:

(a) Rigorous impedance fit

The three components of the impedance Z (C , θ and σ), can be fitted to the measured impedance spectrum according to eqn. (7). The procedure starts by adopting values for the three parameters and searches for the minimum of the error sum χ^2 defined according to:

$$\chi^2 = \sum_i (Z_{i,\text{measured}} - Z_{i,\text{calculated}})^2 \quad (15)$$

where i covers the angular frequencies measured. We usually have 25 separate frequencies, ranging from 5 to 2000 rad s^{-1} . We use this approach in combination with a Newton-Raphson program on a DEC-10 computer. This method gives a good fit, but in the calculation quite some emphasis is put on the lower frequencies. This results in somewhat higher C values than those obtained using other methods (to be described below), and sometimes a charge-transfer resistance is found that does not appear with other methods. In most cases, however, θ is found to be zero. For an example of a measured curve and a set of calculated points see Fig. 7.

We ascribe the non-systematic presence of θ to experimental errors that may be present especially in the low frequency range. Another confusing factor may be the

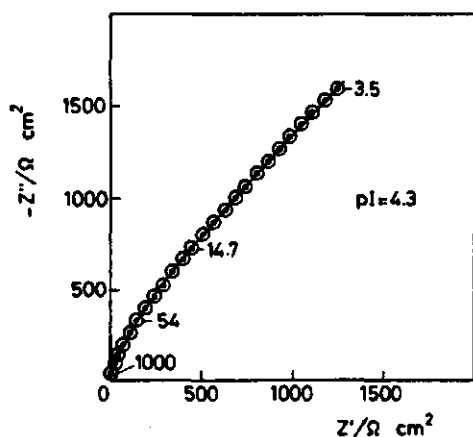


Fig. 7. Impedance spectrum for the AgI/solution electrode, (●) measured, (○) calculated according to fit (a). Parameters: $\theta = 56 \Omega \text{ cm}^2$, $\sigma = 3160 \Omega \text{ cm}^2 \text{ s}^{-1/2}$, $C = 29 \mu\text{F cm}^{-2}$; inert electrolyte 0.1 M KNO₃; angular frequencies are indicated.

influence of surface roughness on the Warburg coefficient, as described in the previous section. As is illustrated in Fig. 5, the shape of the $Z'-Z''$ plot for a rough electrode (filled symbols) differs from the spectrum of a flat one (open circles). If an apparently flat electrode exhibits minor roughness, the fit to the Randles impedance will be worse, but the $Z'-Z''$ plot does not clearly show the (minor) deviations. All the findings mentioned have kept us from trying to improve the rigorous fit method, e.g. by applying weighting factors in the error sum.

(b) Separation of the faradaic impedance Z_F

Separation of the faradaic and capacitive parts of the impedance, as described by Peverelli and Van Leeuwen [6], is an iterative method. It is based on an estimate of C and subsequent calculation of Z_F from the measured spectrum. For technical details the reader is referred to ref. 6. The method yields the real and imaginary parts of Z_F (Z'_F and Z''_F , respectively), and these are plotted separately against $\omega^{-1/2}$. Figure 8 shows an example of such a Randles plot. By linear regression, two straight lines are fitted to the data for Z'_F and Z''_F . The slopes of the two lines, which should be identical, give σ ; the intercept of Z'_F is θ . This plot yields relatively stable σ values, although the plots are not always perfectly straight and parallel, and Z''_F does not always pass through the origin. The resulting θ values are unstable and their dependence on Ag⁺ (or I⁻) solution activity is casual, not systematic. They do not coincide with the irregular θ values obtained by method (a). We ascribe the instability of this procedure to the fact that θ is sensitive to small changes in the slope of the plot. We conclude that the θ values are not reliable, and we anticipate that quite different θ 's could be obtained if different analysis procedures or modified equivalent circuits were applied. The resemblance between the σ and C

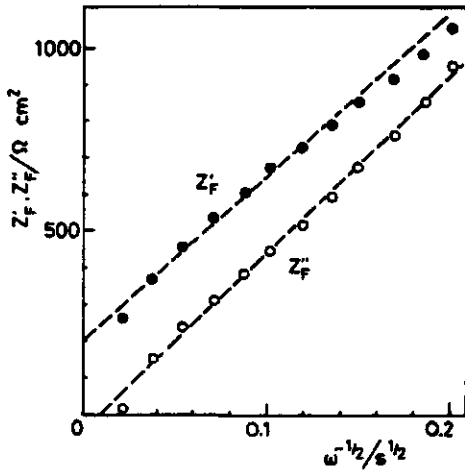


Fig. 8. Real and imaginary components of the Faradaic impedance vs. $\omega^{-1/2}$. $pI = 4.5$, inert electrolyte $0.1 M KNO_3$.

values from this method and those produced by the other methods described here is reasonable.

(c1) Admittance analysis: real component

From the admittance equation (8) it can be seen that:

$$\frac{\omega^{1/2}}{Y'} = \theta \omega^{1/2} + \sigma + \frac{\sigma^2 \omega^{-1/2}}{\theta + \sigma \omega^{-1/2}} \quad (16)$$

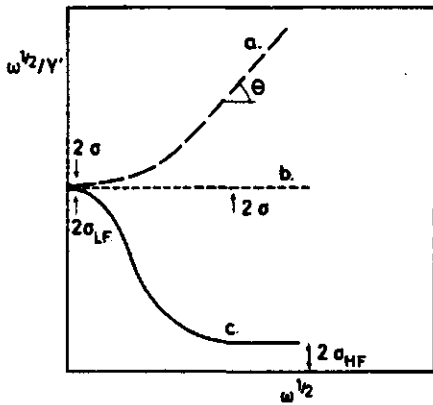


Fig. 9. Plot of $\omega^{1/2}/Y'$ vs. $\omega^{1/2}$ for: (a) $\theta \neq 0$ (---), (b) $\theta = 0$ (- - - - -) (both for flat electrode), (c) rough electrode when $f_R = 6$ and $\theta = 0$ (—).

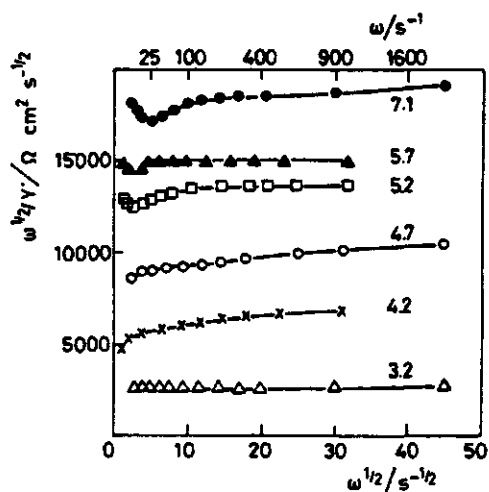


Fig. 10. Plot of $\omega^{1/2}/Y'$ vs. $\omega^{1/2}$ for flat AgI electrodes. 0.1 M KNO_3 ; pl values are indicated.

and a plot of the left-hand side vs. $\omega^{1/2}$ should either show an increase with ω , with slope θ for higher frequencies, or a horizontal line with intercept 2σ (when charge transfer is negligible), respectively shown in Fig. 9, curves a and b. The graphs obtained from our experimental data appear to be essentially horizontal. There is no trace of a significant contribution of θ (see Fig. 10). The values for σ are quite reproducible and compare reasonably well with those calculated according to eqn. (6).

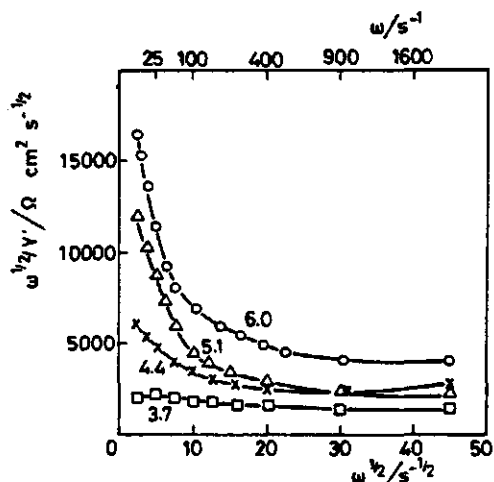


Fig. 11. Plot of $\omega^{1/2}/Y'$ vs. $\omega^{1/2}$ for electrolytically grown ("rough") AgI electrodes. pl values are indicated; 0.1 M KNO_3 .

A serious complication in this procedure is caused by surface roughness. If the electrode surface possesses irregularities of the order of magnitude of the diffusion layer thickness, the plot should show the transition from the low frequency (high level) to the high frequency (low level) value for σ . This was discussed in a preceding section and is illustrated in Fig. 9, curve c.

To investigate this point we have studied electrodes with a high degree of roughness (see the Experimental section and Fig. 2). In Fig. 11 we present $\omega^{1/2}/Y'$ plots for several pI's for these rough electrodes. Especially at low iodide concentrations, where the faradaic relaxation takes place at the lowest frequencies, the plot decreases strongly with increasing ω . The σ values at the lowest ω are comparable to those obtained for (essentially) flat electrodes. Combining these values with the high frequency limits according to eqn. (13) gives us a roughness factor of ca. 5. The characteristic size of the irregularities, ca. 3 μm , corresponds reasonably well with the observation that the transition is in the frequency region around 25 rad s^{-1} .

This experimental evidence on the effect of electrode roughness in admittance plots is in agreement with the work of Oomen [2]. He reported the surface of his electrolytically grown AgI electrodes to be rough, and estimated an f_R of ca. 4, based on capacitance measurements. From the rather few impedance data of Oomen we calculated $\omega^{1/2}/Y'$ plots, which clearly decrease as shown in Fig. 12. Unfortunately, the frequency range is too narrow to cover the whole "roughness spectrum", so we cannot estimate the roughness factor from these data. In two recent publications Kvastek and Horvat [8] described the impedance of a silver iodide electrode consisting of electrolytically deposited AgI on a spherical silver substratum. They presented strongly decreasing $\omega^{1/2}/Y'$ vs. $\omega^{1/2}$ plots, which closely resemble our results for rough AgI electrodes as shown in Fig. 11. Our direct comparison with flat AgI electrodes shows that the decrease in $\omega^{1/2}/Y'$ with increasing frequency is

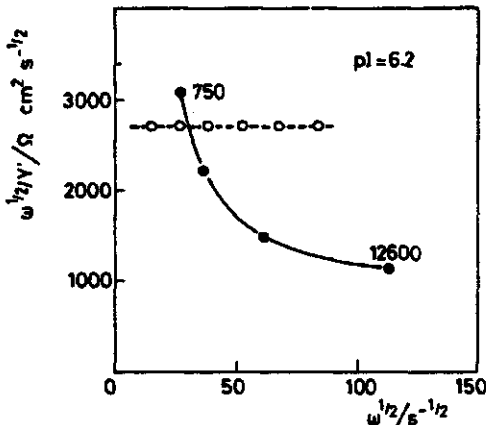


Fig. 12. Plot of $\omega^{1/2}/Y'$ vs. $\omega^{1/2}$. (●) Calculated from the data of Oomen [2], angular frequencies are indicated; (O) result of best fit to the data of Oomen using the Randles circuit (for flat surface). parameters: $\theta = 0 \Omega \text{ cm}^2$, $\sigma = 1340 \Omega \text{ cm}^2 \text{ s}^{-1/2}$, $C = 23 \mu\text{F cm}^{-2}$.

caused by roughness effects. The analysis shows equally well that flat AgI electrodes behave according to the Randles circuit with $\theta = 0$. The resemblance between the behaviour of $\omega^{1/2}/Y'$ for a rough electrode and its behaviour in the case of specific adsorption of electroinactive species [1], is accidental.

We conclude that plotting $\omega^{1/2}/Y'$ as a function of $\omega^{1/2}$ is a helpful device for calculating the Warburg coefficient, and it also provides us with a check on surface roughness.

(c2) *Admittance analysis: imaginary component*

From eqn. (8) it follows that:

$$Y''/\omega = \frac{\sigma\omega^{-1/2}}{\omega(\theta + \sigma\omega^{-1/2})^2 + \sigma^2} + C \quad (17)$$

If θ is non-zero, the graphs of Y''/ω vs. $\omega^{-1/2}$ should show an upward tendency in the high frequency region. In practice this never occurred, which we consider evidence for the insignificance of θ values produced by other methods, e.g. (a) and (b). If θ is negligible eqn. (17) reduces to:

$$Y''/\omega = \omega^{-1/2}/2\sigma + C \quad (18)$$

So for $\theta = 0$ the plot of Y''/ω vs. $\omega^{-1/2}$ is a straight line with intercept C and slope $(2\sigma)^{-1}$. Experimentally, the predicted straight lines were usually obtained, with quite stable and reproducible σ and C values. A few examples are given in Fig. 13. The capacitance values compare well to those obtained by method (b). The agreement with capacitances from titration experiments is rather good, as we will illustrate elsewhere [15]. Furthermore, the σ values are close to those resulting from the analysis of the real admittance, so we conclude that the combined analysis of the real and imaginary admittance is a consistent method for the interpretation of our AgI impedance data.

As expected, the Y''/ω plot is seriously influenced by surface roughness, as can be seen in Fig. 14, showing this plot for a pair of rough electrodes. The graph is curved due to the transition from σ_{HF} to higher values of σ , eventually reaching the value of σ_{LF} . A quantitative interpretation of these curved Y''/ω plots is not yet available. We agree with De Levie's statement that the Randles circuit is not obeyed in the frequency region where the diffusion layer thickness and the "pore" size are of the same order of magnitude [25].

As a first approach, we assume a very simple expression for the frequency-dependent Warburg coefficient, describing qualitatively the S-shape of the $\omega^{1/2}/Y'$ plots:

$$\sigma(\omega) = (1 + f_R \cdot \omega_R/\omega)/(1 + \omega_R/\omega) \quad (19)$$

$\omega_R = \pi D_i/l_R^2$ is the characteristic angular frequency which is related to the size of the irregularities according to $\delta \approx l_R$. The plot of Y''/ω vs. $\omega^{-1/2}$ for frequency-dependent σ values, calculated by substituting eqn. (19) into eqn. (18), shows a com-

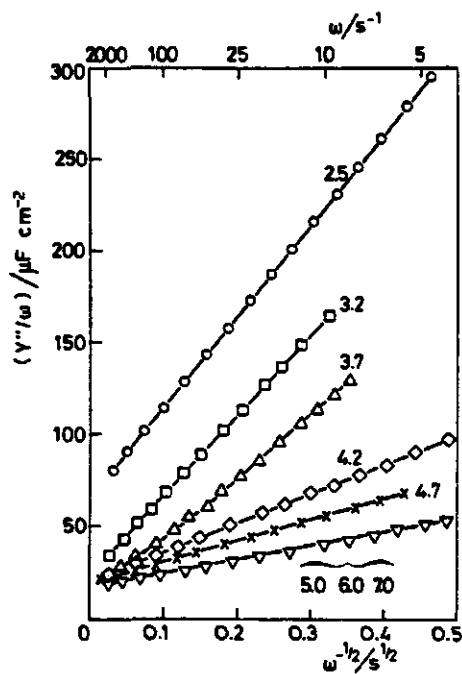


Fig. 13. Plot of Y''/ω vs. $\omega^{-1/2}$ for flat AgI electrodes. $0.1 M KNO_3$; pI values are indicated.

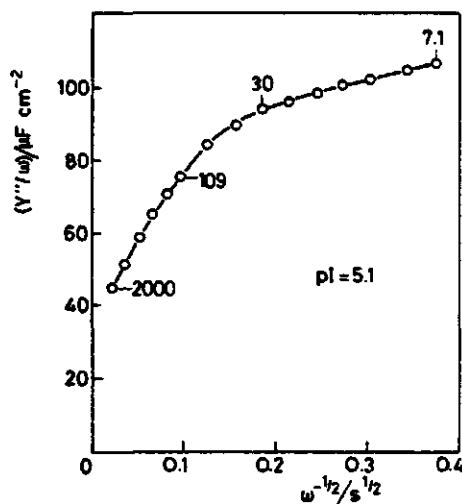


Fig. 14. Plot of Y''/ω vs. $\omega^{-1/2}$ for a rough electrode, experimental. pI = 5.1, $0.1 M KNO_3$, $f_R = 5$, $l_R = 3 \mu m$, angular frequencies are indicated.

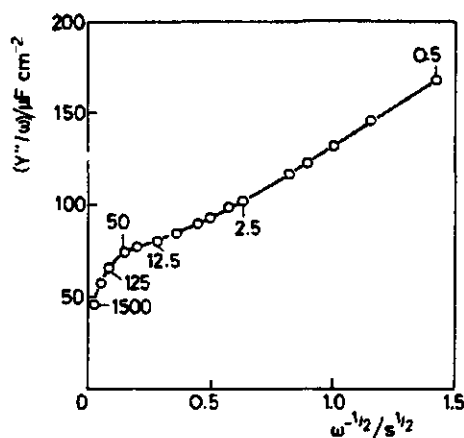


Fig. 15. Plot of Y''/ω vs. $\omega^{-1/2}$ for a rough electrode, calculated according to eqn. (16). Parameters: $\omega_R = 10 \text{ s}^{-1}$, $\sigma_{HF} = 1100 \Omega \text{ cm}^2 \text{ s}^{-1/2}$, $C = 35 \mu\text{F cm}^{-2}$, $f_R = 5.0$.

plicated shape. In Fig. 15 it can be seen that the slope gradually changes over a wide frequency range.

Returning to our experimental data (Fig. 14), we can give the following explanations. The low-frequency part of the plot cannot be used for the evaluation of any σ value, since it represents some transition region between high and low frequency limiting behaviour. The high frequency part tends to a straight line, but we found it risky to extract C and σ values. Practically, this curve has a diagnostic value, being indicative of interference from surface roughness.

CONCLUSIONS

Method of analysis

The assessment of different methods of analysing AgI/solution impedance spectra allows us to draw some pertinent conclusions:

The *rigorous impedance fit* (method a) suffers from low transparency. The $Z'-Z''$ plots for different values of the parameters are not easily distinguishable. The method is numerical by nature, not very suitable for visual examination. This method does not allow easy recognition of surface roughness as a complicating factor and this may lead to erroneous conclusions. For an AgI electrode it yields C values which are too high and non-zero θ values which are not systematically related to experimental conditions.

The *faradaic impedance method* (b) exhibits low transparency, like method (a), because of the involved iteration procedure. It suffers from apparent systematic errors, and produces unstable and erroneous values for the kinetic parameter θ .

The *admittance analysis* (c) has the advantage that it can easily be visualized. If

charge transfer resistance contributes significantly, it can clearly be detected in the real component. The effect of surface roughness, which is a crucial aspect of the AgI electrode impedance, is clearly shown by both the real and imaginary component. The combined analysis of Y' and Y'' yields stable and reproducible σ and C values.

Our ultimate conclusion on the methods is that for the AgI electrode the admittance analysis is to be preferred over impedance analysis. The simultaneous analysis of the spectra of Y' and Y'' provides consistent results and allows a clear diagnosis of effects related to surface roughness, especially in the absence of charge-transfer resistance.

Electrodynamics of the AgI / aqueous solution interface

The results mentioned above allow us to draw the following conclusions concerning the AgI/solution interfacial impedance.

The roughness of the AgI electrode surface may seriously complicate the impedance spectrum, especially as regards the mass transport impedance. Hence the preparation and characterization of the electrode (surface) is important. In the frequency range where the effective diffusion layer thickness for mass transport to or from the solution has the same order of magnitude as the dimensions of the irregularities on the rough AgI electrode surface, the Warburg impedance shows a transition. At the high frequency side of this transition the Warburg parameter is related to the real, microscopic surface area, and at the low frequency side it is related to the geometric surface area.

The electrodynamics of the AgI/solution interface are completely described by a double-layer capacitance and a diffusional impedance, the interfacial ion transfer being fast. The double-layer capacitance values ensuing from our experiments agree reasonably well with those obtained from titration experiments. For flat electrodes the diffusion parameter is close to values calculated from semi-infinite diffusion equations. For rough electrodes the low frequency diffusion parameter is in agreement with the values calculated from these equations when the geometric surface area is taken into account.

ACKNOWLEDGEMENT

The skilful and kind assistance of Mr. Felix Thiel of the Technical and Physical Engineering Research Service in preparing the electron micrographs is gratefully acknowledged.

REFERENCES

- 1 M. Sluyters-Rehbach and J.H. Sluyters in A.J. Bard (Ed.), *Electroanalytical Chemistry*, Vol. 4, Marcel Dekker, New York, 1970, p. 1.
- 2 J.J.C. Oomen, Ph.D. thesis, Utrecht, 1966.
- 3 D.J.C. Engel, Ph.D. thesis, Utrecht, 1968.
- 4 J.H.A. Pieper, Ph.D. thesis, Utrecht, 1976; D.A. de Vooyo, Ph.D. thesis, Utrecht, 1976; J.H.A. Pieper and D.A. de Vooyo, *J. Electroanal. Chem.*, 53 (1974) 243.
- 5 K.J. Peverelli and H.P. van Leeuwen, *J. Electroanal. Chem.*, 99 (1979) 151.
- 6 K.J. Peverelli and H.P. van Leeuwen, *J. Electroanal. Chem.*, 110 (1980) 119, 137.
- 7 K.J. Peverelli, Ph.D. thesis, Wageningen, 1979.
- 8 K. Kvastek and V. Horvat, *J. Electroanal. Chem.*, 130 (1981) 67; 147 (1983) 83.
- 9 B.H. Bijsterbosch and J. Lyklema, *Adv. Colloid Interface Sci.*, 9 (1978) 147.
- 10 J. Lyklema, *Pure Appl. Chem.*, 52 (1980) 1221.
- 11 J. Lyklema and H.P. van Leeuwen, *Adv. Colloid Interface Sci.*, 16 (1982) 127.
- 12 E.P. Honig and J.P.M. Huybregts, *Proc. 33rd ISE Meeting, Lyon (1982)*, 825; E.P. Honig and J.H.Th. Hengst, *J. Colloid Interface Sci.*, 31 (1969) 545.
- 13 S.K. Bose and S.C. Sircar, *J. Mater. Sci.*, 11 (1976) 129; C. Tubandt, *Z. Anorg. Allg. Chem.*, 115 (1920) 113; S.W. Kurnick, *J. Chem. Phys.*, 20 (1952) 218; H. Hoshino and M. Shimoji, *J. Phys. Chem. Solids*, 35 (1974) 321.
- 14 H.P. van Leeuwen in A.J. Bard (Ed.), *Electroanalytical Chemistry*, Vol. 12, Marcel Dekker, New York, 1982, p. 159.
- 15 R.B. Polder, B.H. Bijsterbosch and H.P. van Leeuwen, *J. Electroanal. Chem.*, submitted.
- 16 R.B. Polder, Ph.D. thesis, Wageningen, 1984.
- 17 H.A. Hoyen, Jr. and Y.T. Tan, *J. Colloid Interface Sci.*, 79 (1981) 525.
- 18 B. Timmer, Ph.D. thesis, Utrecht, 1968.
- 19 K.J. Vetter, *Elektrochemische Kinetik*, Springer-Verlag, Berlin, 1961.
- 20 B. Timmer, M. Sluyters-Rehbach and J.H. Sluyters, *J. Electroanal. Chem.*, 14 (1967) 181.
- 21 M.A. Ladjouzi, Ph.D. thesis, London, 1979.
- 22 W. Lorenz, *Z. Elektrochem.*, 58 (1954) 912.
- 23 R. de Levie, Ph.D. thesis, Amsterdam, 1963.
- 24 R. de Levie, *Electrochim. Acta*, 10 (1965) 113.
- 25 R. de Levie in F. Delahay (Ed.), *Advances in Electrochemistry and Electrochemical Engineering*, Vol. 6, Interscience, New York, 1967, pp. 329 ff.
- 26 K.J. Vetter ref. 19, p. 318.

Chapter IV.

ELECTRODYNAMICS OF THE AgI/SOLUTION INTERFACE.

EFFECT OF SOLUTION COMPOSITION AND OF ADSORBED POLYMER.*

1. Abstract.

It is shown that over a wide potential range the impedance of the AgI/aqueous solution interface can be represented by a parallel arrangement of a double layer capacitance C and a diffusion impedance Z_W . The validity of this scheme is neither affected by the addition of ethyleneglycol to the solution, nor by the presence of adsorbed polymer at the interface. Values for C obtained from analysis of the electrode impedance spectrum compare well with those obtained from potentiometric titrations of suspensions. For aqueous solutions Z_W is identified as the Warburg impedance for semi-infinite linear diffusion of Ag^+ or I^- -ions, although for I^- the agreement between measured and calculated values is less than for Ag^+ . In the presence of ethyleneglycol and the polymers PVA and PVP, C is reduced. In the presence of adsorbed polymers Z_W is increased, especially at relatively negative potentials. These results are discussed in terms of the structure of the interfacial double layer and the adsorbed polymer layer.

2. Introduction.

The study of electrodynamics of solid/liquid interfaces has attracted attention for various reasons, among which is its impact on colloid stability. This latter interest is raised by the important question, whether the collision of two colloidal particles in a sol takes place under conditions of constant potential or of constant charge [1, 2]. The former case requires complete relaxation of the electrical double layer at the particle/solution interface during the collision; the latter may be applicable if charge transfer and/or mass transport processes are slow compared to the duration of the collision.

* Submitted for publication in J.Electroanal.Chem., in coauthorship with Bert H.Bijsterbosch and Herman P.van Leeuwen.

In colloid chemical studies, especially silver iodide has extensively been used as a model system. Suspensions as well as electrodes can be prepared with reproducible properties [3, 4]. Another reason for studying silver halide is that its electrical properties have practical relevance for photography, where silver halide (mostly bromide) particles are the light sensitive elements. For this application the adsorption of organic material is of great importance: stabilizer, sensitizer and dye molecules are adsorbed on the particles to enhance stability and sensitivity, in order to improve the spectral response and to enable colour photography [5].

A lot of work has been done with **suspensions** of AgI, mainly in the form of titration experiments. These experiments provide surface charge-potential relations, which subsequently can be converted into capacitance-potential dependencies. Among these studies are those where organic material was present at the interface, either as small molecules like alcohols [6, 7], or as large polymer molecules [8, 9]. The nature of titration experiments is static, in the sense that the measurements ultimately provide data under equilibrium conditions.

The study of silver iodide **electrodes** in aqueous solution can reveal electrodynamic properties, such as parameters of ion transfer kinetics [10, 11, 12, 13]. Moreover, the double layer capacitance can be inferred as a function of the potential [14], which is an interesting alternative for obtaining the capacitance-potential relation from titration experiments. Up till now the dynamic experiments on silver iodide have been confined to cases in which no organic material was present at the interface.

A number of authors have described the preparation and characterization of silver iodide electrodes [4, 12, 14]. Recently we have shown how to prepare electrodes which are sufficiently flat to avoid problems related to surface roughness. The impedance spectrum of these electrodes was shown to behave according to a Randles type of circuit [15], including a Warburg diffusion impedance representing the transport of Ag^+ or I^- -ions in solution, and a double layer capacitance which incorporates the adsorption of Ag^+ or I^- . The interfacial transfer of these ions was shown to be fast on the timescale of our measurements, which went down to 0.5 msec [15].

In this paper we will present data on the diffusion parameter and the

double layer capacitance obtained with AgI electrodes in aqueous (mostly 0.1 M) KNO_3 solutions, with or without organic molecules being adsorbed on the electrode surface. Adsorbed substances were ethyleneglycol (EG), as an example of a small surface active molecule, and the polymers poly (vinylalcohol) (PVA) and poly (vinylpyrrolidone) (PVP), as examples of strongly adsorbing large molecules. Titration data on the systems EG/AgI [6], PVA/AgI [8] and PVP/AgI [9] are also available, so that a comparison of the capacitance data will be possible. The consequences for colloid stability will be dealt with in a forthcoming publication [16].

3. Experimental.

a. experimental setup and AgI electrodes.

The cell was a double wall pyrex vessel with inlets for nitrogen, a salt bridge (connected to a reference electrode) and two AgI electrodes. The cell was kept at $25 \pm 0.2^\circ\text{C}$ and was placed in a Faraday cage. Essentially, the whole setup was the same as described by Peverelli and Van Leeuwen [10].

Each of the AgI electrodes consisted of a flat thin layer of AgI, grown by reaction of a massive polished silver substratum with iodine vapour in air (from a iodine solution in ethanol) at room temperature. After completion of the AgI layer, the electrodes were aged for 72 hours at 80°C in a solution of 10^{-3} M KNO_3 and 10^{-4} M KI. The average thickness of the films ranged from 300 to 1000 nm. Scanning electron microscopy revealed the surface of the film to contain irregularities with magnitudes up to 300 nm. It was verified by Electron Backscattering analysis, that the whole electrode surface was covered with AgI, even between the coarsest grains. The microstructure of the AgI surface was displayed in a previous paper [15]. There it was also shown that in the frequency range used ($5 \dots 2000 \text{ rad sec}^{-1}$), these electrodes behave as flat electrodes. For more details on the preparation of the electrodes we refer to a forthcoming publication [16].

The potential of the AgI electrodes with respect to the solution was adjusted by adding small amounts of either KI or AgNO_3 solutions. The relation between concentration and cell potential was calibrated in the range of 10^{-2} to 10^{-5} molar Ag^+ or I^- . For concentrations below 10^{-5} the obtained calibration lines were extrapolated. It may be worthwhile

emphasizing that cell potential E , iodide concentration $c(I^-)$ and silver concentration $c(Ag^+)$ together represent only one variable [3]. The equilibrium potential is related to the Ag^+ activity $a(Ag^+)$ by :

$$E = E^{\circ} + (R T / F) \ln a(Ag^+) \quad (1)$$

or

$$E = E'^{\circ} + (R T / F) \ln c(Ag^+) = E'^{\circ} - (2.3 R T / F) pAg \quad (2)$$

where $E'^{\circ} = E^{\circ} + (R T / F) \ln f$ and f is the activity coefficient. Since the equilibrium concentration of iodide ions is determined by the solubility product L and the silver concentration, the latter equation is equivalent to $E = E''^{\circ} - (2.3 R T / F) pI$, with $E''^{\circ} = E'^{\circ} + (R T / F) \ln L$.

We have taken the capacitance of the AgI electrode in 0.1 M KNO_3 solution at $pAg = 10$ as a reference for estimating the roughness factor, f_R , the ratio between the real and geometric surface area. Under these conditions the slope of the capacitance versus potential curves is minimal according to most authors [6, 14, 10, 11, 17]. Besides, the concentration determination around $pAg 10$ is more reliable than around $pAg 8$ ($I^- = 10^{-6}$ vs 10^{-8}). Agreement with literature data is best, when f_R is assessed at 1.5. This approach is reasonable, as illustrated by the fact that Peverelli and Van Leeuwen [14] estimated the same value for electrodes of comparable type.

b. chemicals.

All solutions were made up of "AgI-water", produced by slowly passing demineralized water through a column of precipitated AgI. This process served to remove any surface active substances still present in the water. Care was also taken to remove adsorbable substances from the salt used to make up the electrolyte solutions.

Silver nitrate, potassium iodide and ethyleneglycol were of reagent grade quality and were used without further purification. The poly (vinylpyrrolidone) (PVP) used was a BASF product, with an average molecular weight of about 900,000. The poly (vinylalcohol) (PVA) was a sample prepared by Scholtens [18]. It had a molecular weight of 90,000

and contained 20% acetate groups in a blocky distribution (about 3 to 5 acetate ester groups in a sequence).

The nitrogen, bubbling through the cell solution before experiments, was freed from traces of oxygen. During the actual measurement a nitrogen atmosphere was maintained.

c. adsorption of polymers.

The coverage of the AgI electrode surface with polymer was carried out before experiments were started. During some 20 minutes the electrodes were immersed in a 1000 ppm polymer solution. Subsequently, they were carefully rinsed with AgI-water and placed in the cell.

The adsorption of polymer molecules is known to be almost complete at the employed concentration. Koopal [8] reported a coverage of AgI as high as 85% for PVA at much lower concentrations. The degree of coverage is limited by mutual steric hindrance of the polymer segments (trains) only, so for our experiments we may count with a coverage of the order of 90%. The adsorbed amounts can be expected to be about 0.8 mg m^{-2} for PVA, [8] and 0.5 mg m^{-2} for PVP [9], where it should be noted, that in the estimation of these numbers the specific surface area as inferred from the capacitance is taken into account [8]. For these large polymers it is known, that the molecules, once adsorbed, are bound firmly to the surface, so that they cannot be washed off with water [19]. Therefore it was not necessary that the cell solution contained any polymer. This has the advantage that contamination of the cell by large amounts of polymer is avoided.

d. measuring technique and analysis procedure.

Impedances were measured with the coulostatic impulse method. It involved a short ($< \text{microsec}$) charging impulse applied to two identical electrodes, and subsequent measurement of the resulting potential/time transient. The impedance-frequency spectrum was then obtained by Laplace transformation of the transient [20]. The electrical setup and the transformation procedure were essentially the same as described by Peverelli and Van Leeuwen [10].

The impedance-frequency spectrum was analyzed in terms of the admittance (Y), split up into its real (Y') and imaginary (Y'') components. If the interfacial ion transfer reaction is fast, so that the transfer

resistance can be ignored, the admittance is [21, 22]:

$$Y = (1-j) \omega^{\frac{1}{2}} \frac{1}{2 \sigma} - j \omega C \quad (3)$$

where $j=(-1)^{\frac{1}{2}}$, ω the angular frequency in rad/sec, σ the Warburg coefficient and C the double layer capacitance. Two special admittance functions are used in the analysis :

$$\frac{\omega^{\frac{1}{2}}}{Y'} = 2 \sigma \quad (4)$$

and

$$\frac{Y''}{\omega} = \frac{\omega^{-\frac{1}{2}}}{2 \sigma} + C \quad (5)$$

A plot of $\omega^{\frac{1}{2}}/Y'$ versus $\omega^{\frac{1}{2}}$ thus should provide a horizontal line with value 2σ . In Fig. 1. a few affirmant experimental examples are displayed, obtained for two pAg's, both for the 'clean' electrode and

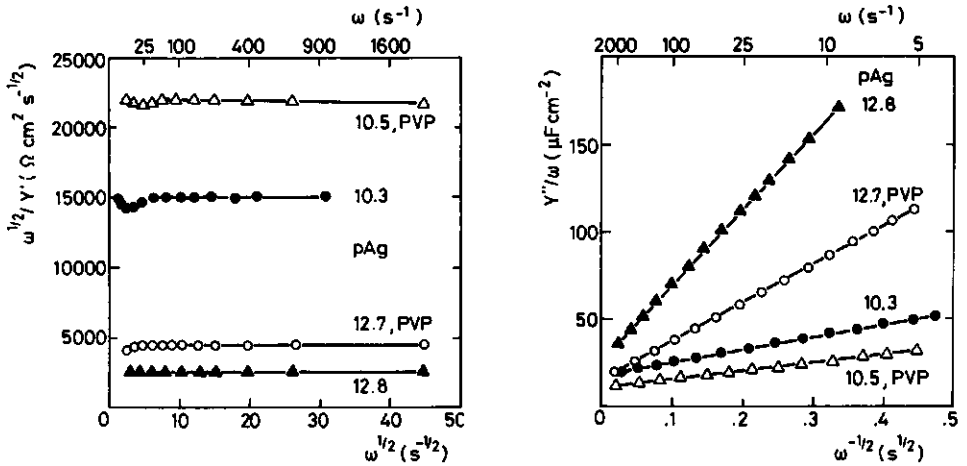


Fig. 1. Plot of $\omega^{\frac{1}{2}}/Y'$ vs $\omega^{\frac{1}{2}}$ for AgI electrodes in 0.1 M KNO_3 solution.

● pAg 10.3, no polymer Δ pAg 10.5, PVP adsorbed.
▲ 12.8, " ○ 12.7, PVP "

Fig. 2. Plot of Y''/ω vs $\omega^{-\frac{1}{2}}$ for AgI electrodes in 0.1 M KNO_3 solution. Symbols have the same meaning as in Fig. 1.

for one with adsorbed PVP. The plot of Y''/ω versus $\omega^{-1/2}$ shows the predicted straight line with slope $1/2\sigma$ and intercept C , as exemplified in Fig. 2.

These results show that the relatively simple scheme comprising a diffusional (mass transport) impedance and a double layer capacitance in parallel also applies when adsorbed polymer is present at the AgI/solution interface. The arguments given in [15] in favour of analysing the impedance in terms of eq(4) and (5) are still valid, thus justifying this analysis procedure throughout this study.

4. Results and discussion.

a. KNO_3 solutions

Fig. 3. shows the differential double layer capacitance C of the AgI/ aqueous solution interface as a function of pAg for 0.1 and 0.01 M KNO_3 .

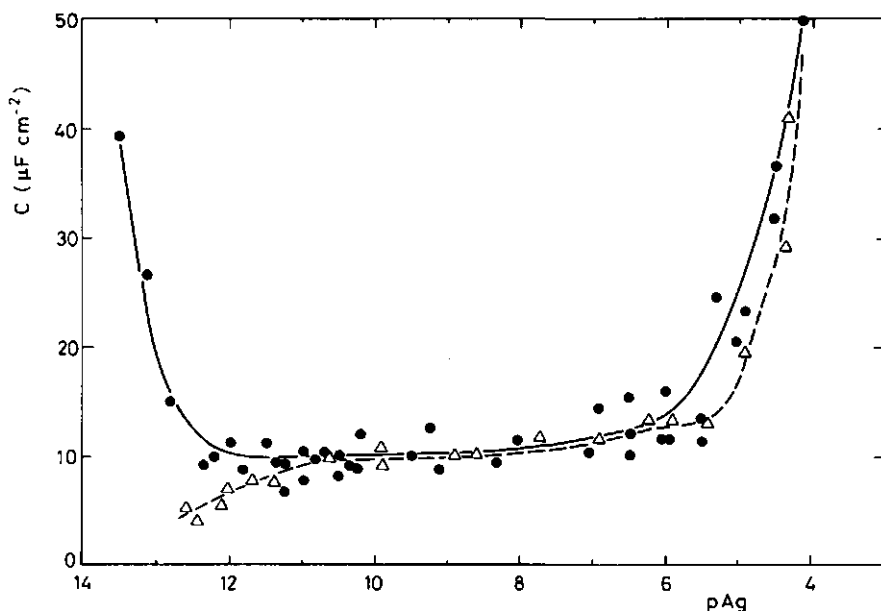


Fig. 3. Differential double layer capacitance of the AgI/ solution interface vs pAg . Temperature 25°C.

● and (—) : 0.1 M KNO_3 . Δ and (----) : 0.01 M KNO_3 .

In the graph for 0.1 M we distinguish three regions: 1. a relatively sharp rise for $pAg > 12$, 2. a sharp rise for $pAg < 6$, 3. a rather flat curve between pAg 12 and 6. The general outline of this capacitance-potential dependency is well known [10,11]. In the range of low concentrations of potential determining ions, say between pAg 6 and 12, the capacitance is roughly constant. This is in agreement with the following, rather simple, picture of the double layer: a. in 0.1 M I^{-1} electrolyte the double layer capacitance is predominantly governed by the Stern layer, b. the Stern layer capacitance behaves as a plate capacitor: its thickness and dielectric constant being nearly independent of the potential difference or the charge density.

Outside this region the capacitance depends on the potential. It is known that for pAg below 5 the capacitance is lower in 0.1 M KF solution than in 0.1 M KNO_3 solution [3]. As fluoride is considered to be practically non-adsorbing, the rise of C can be attributed to the co-adsorption of nitrate at low pAg [3]. This specific adsorption of anions facilitates the adsorption of Ag^+ , thus leading to apparently high charges. This picture is confirmed by the observation that in this potential region the electrophoretic mobility is rather low, and sols are relatively unstable [3], considering the apparently high surface charge densities. Note that in studies on dispersions the surface charge is evaluated from the variation in the difference in adsorbed amounts of $AgNO_3$ and KI.

At $pAg > 12$ the rise of the capacitance must be attributed to co-adsorption of cations. This is in line with the observation that there is a lyotropic effect on the capacitance for negatively charged silver iodide [3,23,24,25]. Rb^+ ions with higher polarizability and lower degree of hydration give a considerably higher C than Li^+ ions. This points towards specific adsorption as the cause of the lyotropic effect. A detailed study of double layer properties of AgI in water and EG-water mixtures has shown the specific adsorption of K^+ at negative surfaces [26]. We have checked the influence of adsorbing ions by a few experiments with Tl^+ ions, which are known to adsorb strongly. Addition of 0.001 M $TlNO_3$ (to 0.1 M KNO_3) resulted in an increase of the capacitance by a factor of two in the pAg range between 10 and 11.5.

For 0.01 molar KNO_3 (the dashed curve in Fig. 3) the shape is somewhat different: 1. for $pAg > 11$ the curve continues to decrease. 2.

for $4 < pAg < 6$ the capacitance is lower than for 0.1 M, but near pAg 4 the rise is very steep again. 3. between pAg 6 and 11 the curve for 0.01 molar coincides with the one for 0.1 M.

The differences between the two ionic strengths occur where the 0.1 M curve is bending upward. The lower capacitances for 0.01 M as compared to those for 0.1 M at $pAg < 6$ may originate from a less pronounced co-adsorption of nitrate in the case of 0.01 M. Another possible explanation is that the relative importance of the diffuse part of the double layer around pAg 5.5 for 0.01 M salt is greater than it is for 0.1 M. The diffuse double layer capacitance has the shape of a parabola with the minimum at the p.z.c. The contribution of the diffuse capacitance might be seen in the lowered capacitance around pAg 5.5. Experiments in 0.001 M KNO_3 have shown the existence of a minimum at the p.z.c. [14], resulting from the complete dominance of the diffuse layer at this low electrolyte concentration. In our experiments its influence, however, is small.

The decrease for $pAg > 11$ may be explained by the less complete screening of the surface charges, as compared to 0.1 M. As $[K^+]$ is lower, co-adsorption is lower. The interaction of negatively charged sites at high surface charge densities may hinder the charge to increase, so the capacitance decreases. The same effect is seen in the charge-potential curves, which tend to level off around pAg 11 [3].

In Fig. 4. we present our data, together with those obtained from coulostatic pulse transients by Peverelli et al. [10,11], data of De Wit [6] obtained by titration experiments, and of Engel [17] and Pieper and De Vooy [14] from bridge impedance measurements. The KNO_3 concentration was always 0.1 M. Literature data are pictured by symbols only for the sake of clarity. Qualitatively our results agree with literature capacitance data, quantitatively there are some differences. It must be stressed here that problems in estimating the roughness factor (electrodes) or the specific surface area (sols) cause inaccuracies in the scaling of the data.

The differences between our results and those of Peverelli et al. originate from the somewhat different analysis of the relaxation data. At low and high pAg values the faradaic impedance has very low values. If the faradaic analysis procedure is used this will decrease the accuracy of the capacitance evaluation, because of its more involved

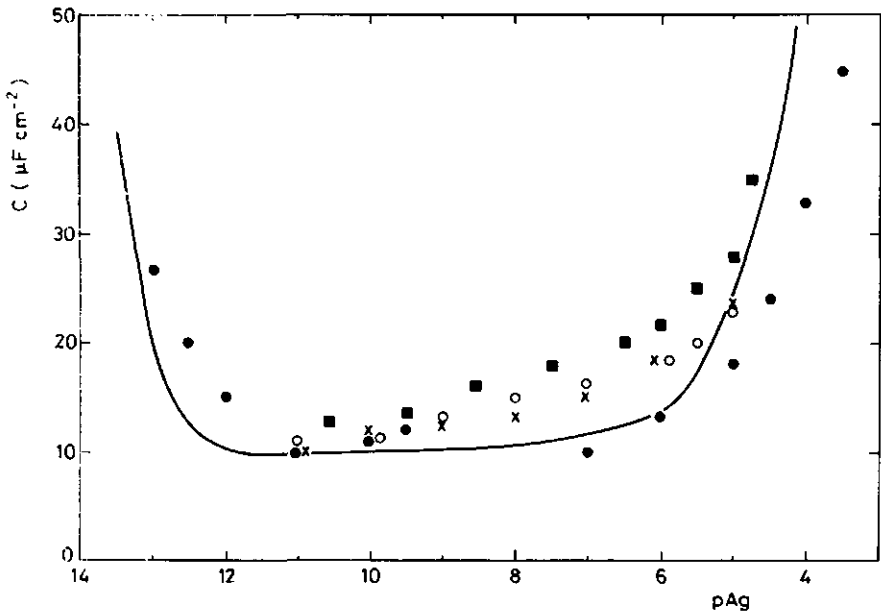


Fig. 4. Double layer capacitance vs pAg. Electrolyte for all experiments: 0.1 M KNO_3 . ● Peverelli et al. [10]; ■ Pieper et al. [14]; × De Wit [6]; ○ Engel [17]; (—) this work.

nature compared to the (total) admittance analysis we have applied.

Most striking difference between our results and titration data is the slow decrease of C with increasing pAg in the middle region, where our C is nearly constant. As mentioned, for $\text{pAg} > 12$ and $6 > \text{pAg} > 4$, our results for 0.01 M show a lower capacitance than for 0.1 M. In Fig. 5, the same tendency is seen in the data of Peverelli et al.; however, the data completely coincide in the region from pAg 5.5 to 12.5 on. For the range of pAg 6 to 10 the same applies as with 0.1 M: small differences between Engel's work and that of Pieper et al. and this work must be attributed to uncertainties in estimating the roughness factor.

In Fig. 6. the log of the Warburg coefficient σ is plotted vs pAg for both electrolyte concentrations. Three different regions can be observed: 1. for $\text{pAg} > 10.5$ log σ decreases with increasing pAg. Around pAg 11 the 0.01 molar curve lies above the 0.1 M one but the difference gradually disappears towards higher pAg; 2. from pAg 6 on log σ decreases sharply with decreasing pAg, and the curves for the two electrolytes overlap almost completely; 3. from pAg 10 to 6.5 log σ for 0.1

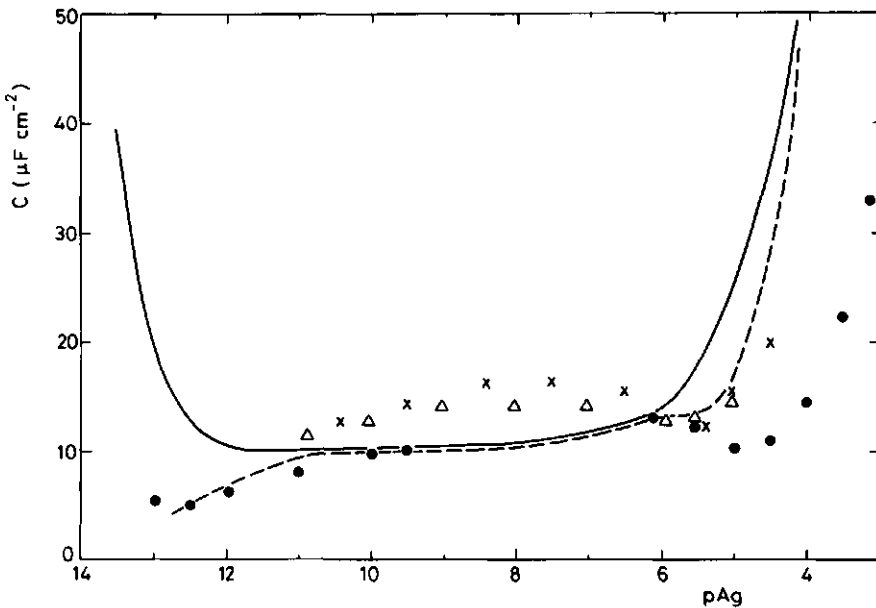


Fig. 5. Double layer capacitance vs pAg. ● Peverelli et al. [11];
 × Pieper et al. [14]; Δ Engel [17]; (-----) this work; All ex-
 periments: electrolyte 0.01 M KNO₃, except (————) this work, 0.1 M.

M KNO₃ is almost invariable, whereas the 0.01 M curve slowly decreases from the higher values around pAg 10 towards the overlap with the 0.1 M plot in the region below pAg 7.

In Fig. 7. we compare our results for the Warburg coefficient with those from literature. Comparison can also be made to σ values calculated from semi-infinite linear diffusion theory according to:

$$\sigma_1 = \frac{R T}{F^2 c_1 (2D_1)^{1/2}} \quad (6)$$

where R, T and F have their usual meaning, and c_1 and D_1 are the concentration and the diffusion coefficient of ion 1 (here Ag⁺ or I⁻) respectively. In Fig. 7. the dashed line at the left side represents σ 's calculated for iodide diffusion, the one at the right those for silver diffusion.

Between pAg 6 and 4 the experimental data are in reasonable agreement with equation (6). This holds for ours as well as those of Peverelli et al. in 0.1 and 0.01 M [10,27], and those of Kvastek and Horvat in 0.01 M

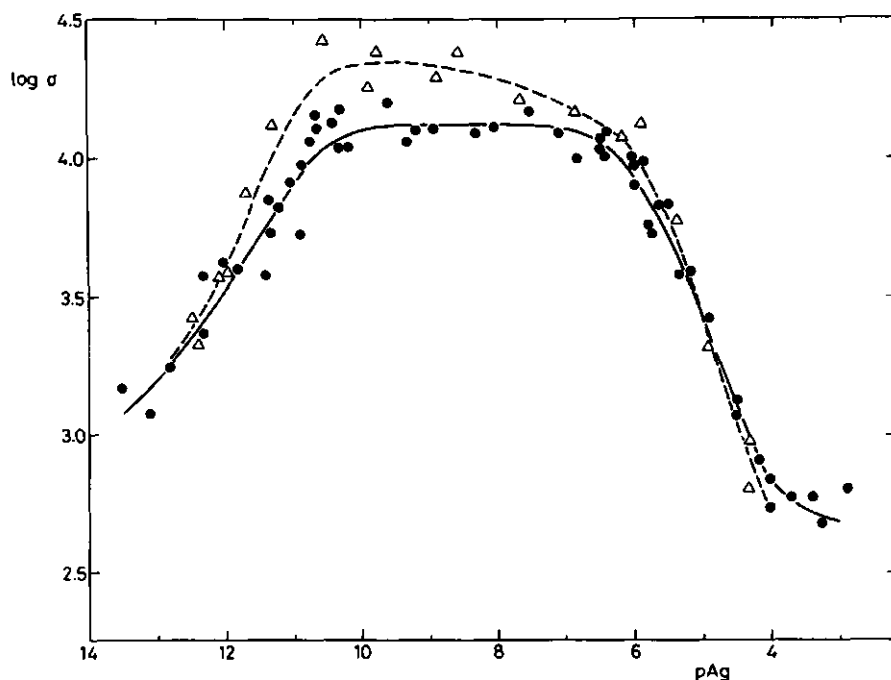


Fig. 6. Warburg parameter σ vs pAg.

● and (—) 0.1 M KNO_3 , Δ and (----) 0.01 M KNO_3 .

KNO_3 [12,13]. We note that the original data of Kvastek et al. (in $\Omega \text{ sec}^{-\frac{1}{2}}$) were normalized to $\Omega \text{ sec}^{-\frac{1}{2}} \text{ cm}^2$. Alternatively one might take the low frequency values from their $\omega^{\frac{1}{2}}/\gamma'$ plots. This procedure provides a more correct measure for the diffusion parameter, as we have explained elsewhere [15]. However, if $\log \sigma$ is taken from the $\omega^{\frac{1}{2}}/\gamma'$ plots, the overall comparison remains roughly the same.

For $\text{pAg} > 11$, the agreement between experiments and theory is less satisfactory, although $\log \sigma$ decreases systematically with increasing pAg (=increasing I^- concentration).

In the region between pAg 6 and 10 σ is nearly independent of pAg. The reason for this discrepancy may be that parameters describing diffusion, being a faradaic process, cannot be measured with sufficient accuracy in this low concentration range. Another cause for the deviation could have been the presence of pseudopotential determining ions, such as Pb^{2+} , Cd^{2+} or Cu^{2+} . By a few DPASV (Differential Pulse Anodic Stripping Voltammetry) experiments we have established the level

of contaminants of the solutions used. The level found could only partly explain the plateau in the $\log \sigma$ curve.

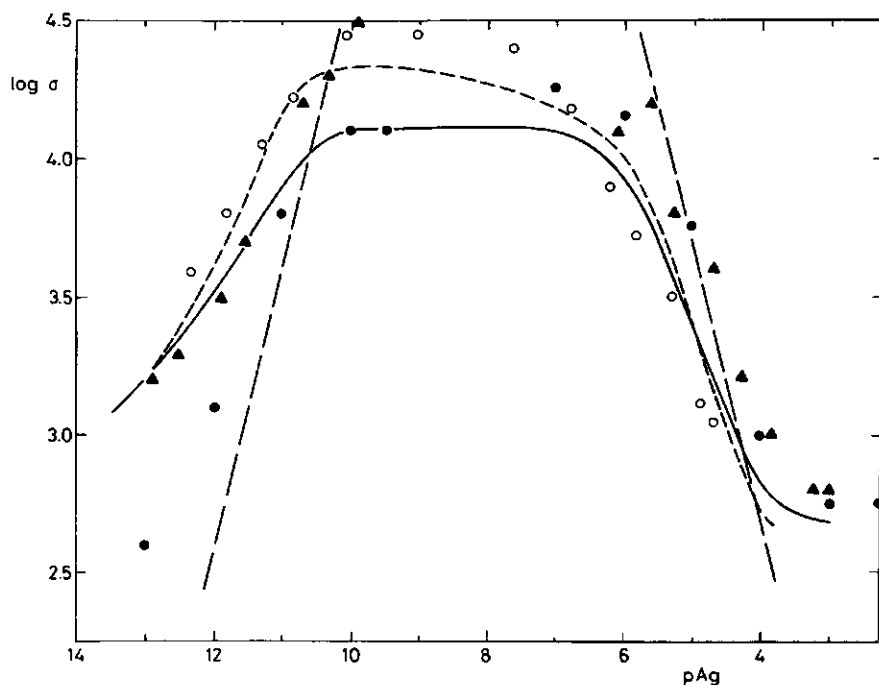


Fig. 7. Warburg parameter σ vs pAg .

● Peverelli et al. [10], 0.1 M KNO_3 , ▲ Peverelli [27], 0.01 M KNO_3 .

○ Kvastek et al., recalculated from [13], 0.01 M KNO_3 .

(——) this work, 0.1 M KNO_3 . (-----) this work 0.01 M KNO_3 ,

(- - -) calculated with eq. (3).

b. water-ethyleneglycol mixture.

In Fig. 8. we show capacitance data obtained for a water EG-mixture with $X_{EG}=0.1$. The general shape of the plot is similar to the EG-free curve, but both for $pAg > 12.5$ and for $pAg < 6.5$ a reduction of C is observed. Direct comparison between De Wits data [6] and our results in the range between pAg 7 and 5 gives close agreement at pAg 5, less agreement at pAg 6, and again better agreement at pAg 7. It should be noted that De Wits curves for EG-free solutions (0.1 M KNO_3) show the same trend, as can be seen in Fig. 4.

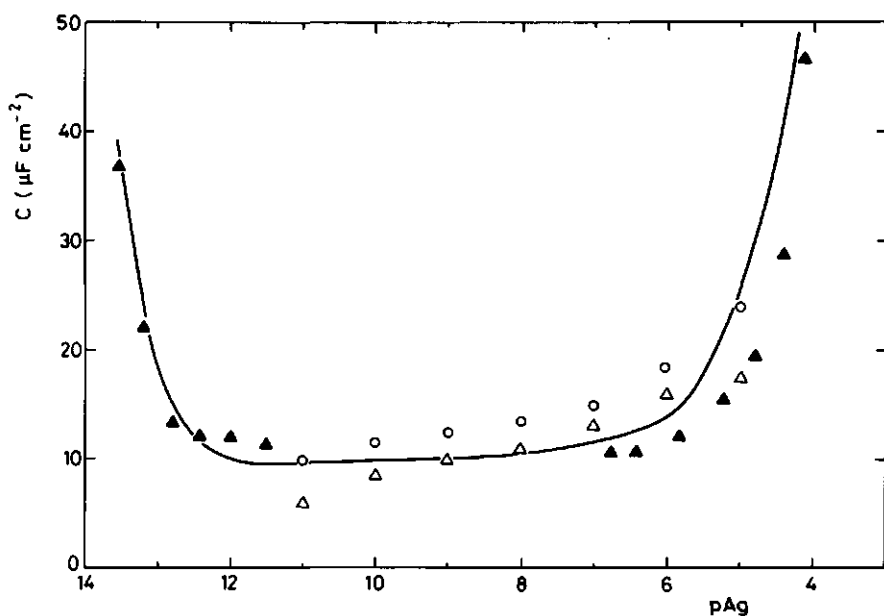


Fig. 8. Double layer capacitance vs pAg.

○ De Wit [6]; (—) this work, both 0.1 M KNO_3 .

△ De Wit [6]; ▲ this work, both 0.1 M KNO_3 and $X_{\text{EG}} = 0.1$.

An overall reduction of the capacitance is generally found when alcohols are adsorbed on silver iodide [3], and it also holds for the system EG-silver iodide, as described by De Wit [6]. It has also been explained that the decrease of C generally has two causes [3]. Firstly, the Stern capacitance decreases because of the decreasing permittivity and an increasing Stern layer thickness. Secondly, the tendency of counterions to get very close to the interface will be reduced because of the lower permittivity, i.e. the degree of (specific) co-adsorption is reduced. De Wit has concluded that in the case of EG/AgI the increase of the Stern layer thickness is the most important factor [6].

The difference between solutions with and without EG with respect to σ is hardly significant. We conclude that diffusion in solution is only little influenced, which is in accordance with the fact that the change of the viscosity and the conductance is not more than a factor of two [6] for the change from water to water-EG with $X_{\text{EG}} = 0.1$.

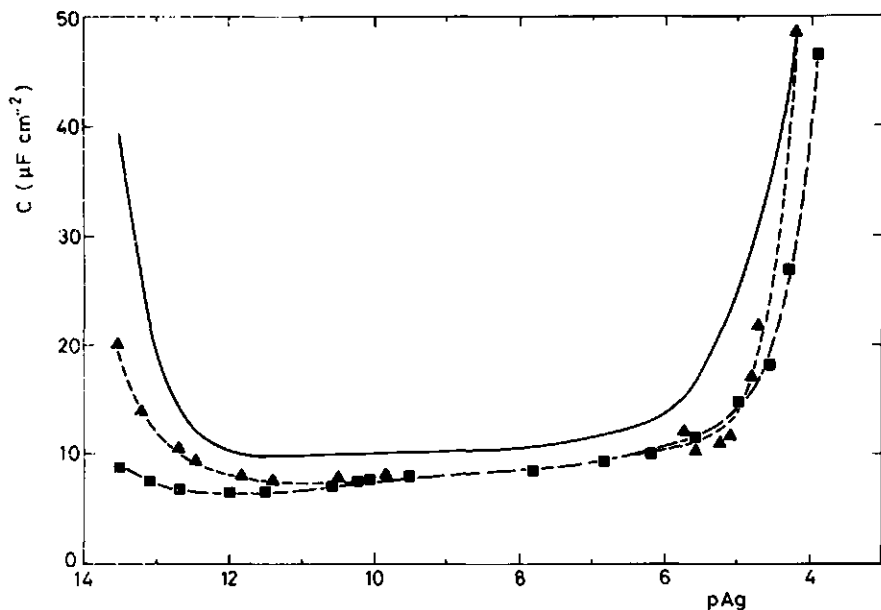


Fig. 9. Double layer capacitance vs pAg. (—) no polymer.
 ■ and (---) adsorbed PVA ($M 9 \cdot 10^4$).
 ▲ and (-----) adsorbed PVP ($M 9 \cdot 10^5$). Electrolyte 0.1 M KNO_3 .

c. interface with adsorbed polymer.

The change in the capacitance due to polymer molecules adsorbed on the electrode surface is much more drastic than for EG. As can be seen in Fig. 9., for both polymers the capacitance is lowered over the complete potential range. In the middle region the level is reduced by some 20 to 30%. For $pAg > 12$ in the presence of PVP the rise of C is much smaller than without polymer; with adsorbed PVA there is hardly any increase at all up to $pAg 13.5$. At the low pAg side, the rise begins at higher Ag^+ concentrations than in the absence of adsorbate; for PVA the curve is below that for the plain electrolyte solution up to pAg about 3.5; with PVP the curve is lower up to $pAg 4.3$.

In Fig. 10. we compare our results for PVA with those obtained by Koopal [8] from titration of AgI suspensions. The graph shows less reduction of C by PVA in our data than in those of Koopal, but the

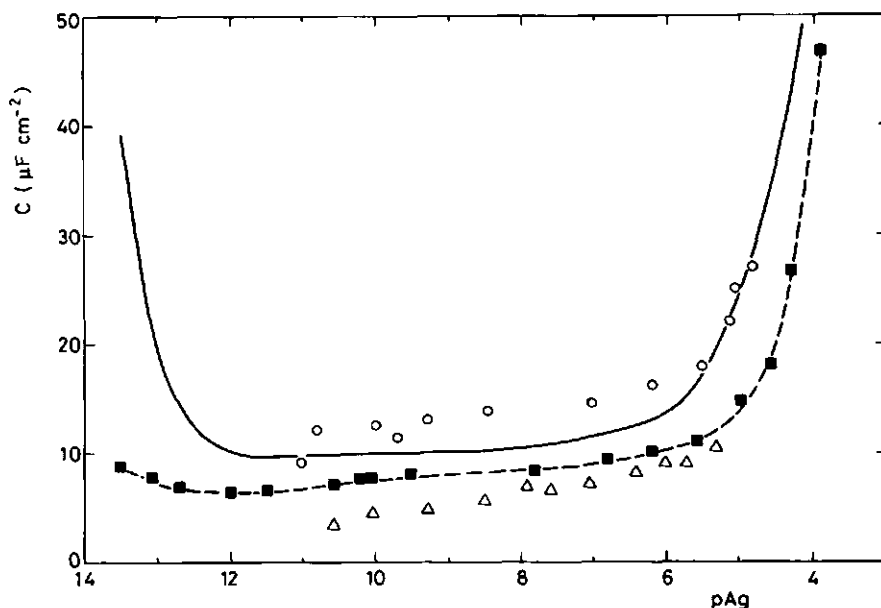


Fig. 10. Double layer capacitance vs pAg. o Koopal, no polymer, calculated from [8]. (—) this work, no polymer. Δ Koopal, 0.5 mg PVA m^{-2} , calculated from [8]. ■ and (-----), PVA adsorbed, this work. All experiments electrolyte 0.1 M KNO_3 .

general trend is the same. The reason for the quantitative difference is not clear. In Koopal's experiment the adsorbed amount of PVA 13-88 was 0.5 mg m^{-2} (based on the capacitance specific surface area). When more PVA was added, the capacitance was not reduced any further, which is in agreement with conditions of almost complete coverage. Koopal has ascribed the reduction of C to either a reduction of the relative (static) permittivity of the Stern layer, or a change in specific adsorption of electrolyte ions. We might add that an increase of the Stern layer thickness resulting from polymer adsorption, would also decrease the capacitance.

A similar trend shows up in the comparison of data on adsorbed PVP. Fig. 11. displays our data and titration data of Van der Schee [9]. His curve for the polymer-free case is at the same level as ours, although towards low pAg it ascends more than ours. For pAg 4.5 to 6 our PVP data are very close to his, whereas for pAg above 8 Van der Schee's values

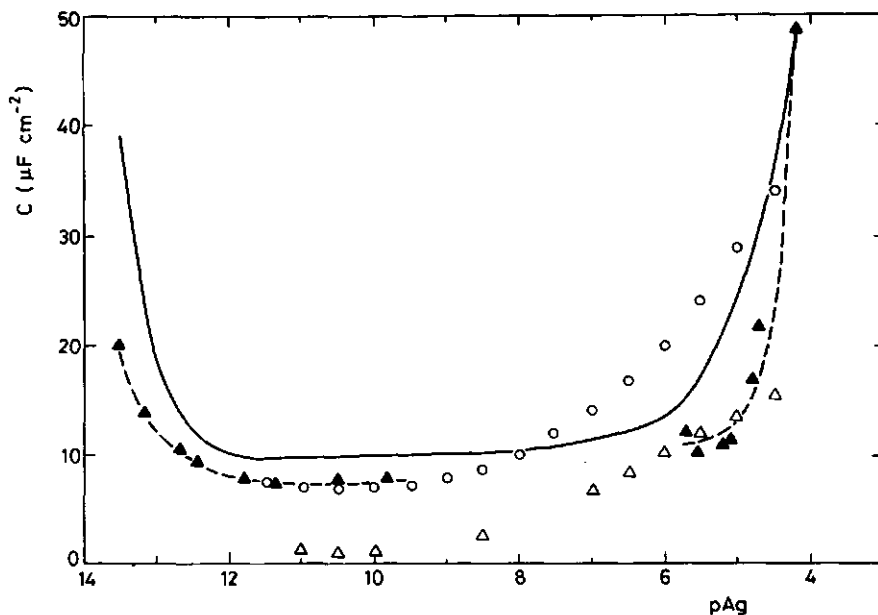


Fig. 11. Double layer capacitance vs pAg.

o Van der Schee, no polymer, calculated from [9].

(——), this work, no polymer.

Δ Van der Schee, PVP adsorbed, calculated from [9].

▲ and (-----), this work, PVP adsorbed.

All experiments electrolyte 0.1 M KNO₃.

are many times lower than our values. Part of the difference is related to the fact that the titration method is less accurate for $pAg > 10$, whereas our experiments give more accurate results for pAg from 10 to 13.5. Principally the same applies to the low pAg part.

Our measurements show the reduction of C to be less with PVP than with PVA, so either PVP has less influence on double layer structure, or its lower impact is simply due to a lower adsorbed amount. Especially at $pAg < 5$, PVP may be expelled to some extent by the co-adsorption of NO_3^- as is suggested by the capacitance which follows the upward trend just like in the polymer-free case. The PVA curve is increasing, but does not reach the same value as the plain curve, unlike the PVP cure. The increase at high pAg for PVP can be attributed to the increasing charge on the surface, but strong desorption of PVP is improbable, as its adsorption maximum is around $pAg 10.5$ [9]. The difference between PVP and PVA is probably due to the lower coverage for PVP, allowing more K^+

to be adsorbed, leading to an increasing C . With PVA this cation adsorption is strongly reduced because of the high degree of coverage, resulting in a low capacitance up to pAg 13.5.

As illustrated by Figs. 1 and 2. the semi-infinite diffusion process still applies with adsorbed polymer, although the value of the diffusion parameter is influenced. Fig. 12. shows that for PVP the change relative to the adsorbate-free system is significant only in the high pAg range. Adsorption of PVA on the other hand, causes the Warburg coefficient to increase considerably over the whole potential range, except for $pAg < 5$. The plateau in the intermediate region is raised and the differences even increase with increasing I^- concentration (from pAg 11 to 13.5).

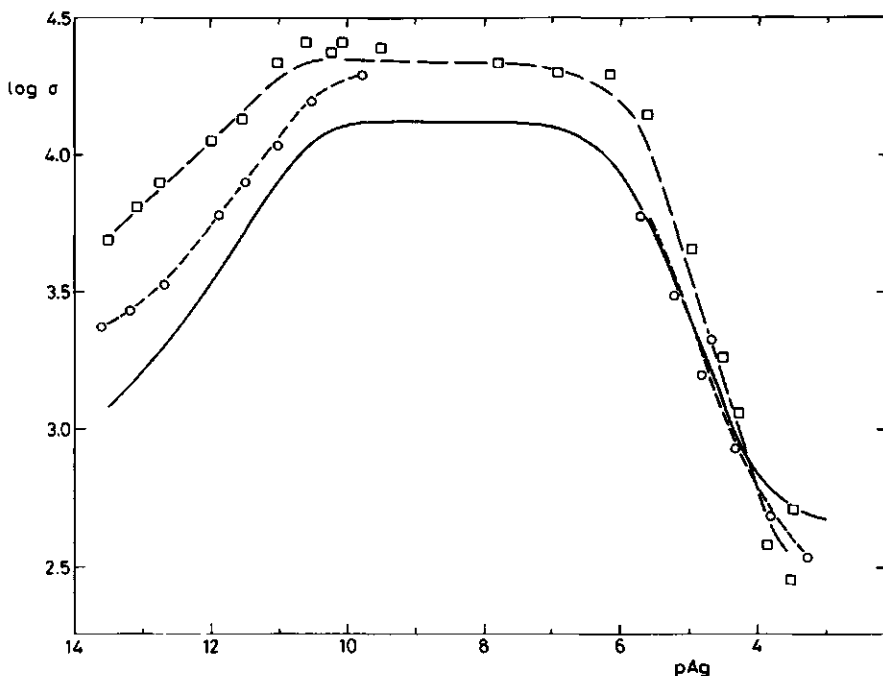


Fig. 12. Warburg parameter σ vs pAg . (—) no polymer.
 \square and (---) PVA adsorbed, $M 9 \times 10^4$.
 \circ and (-----) PVP adsorbed, $M 9 \times 10^5$.
 All experiments electrolyte 0.1 M KNO_3 .

It is most likely that the increase of the Warburg coefficient is caused by a retardation of the diffusional transport of Ag^+ or I^- . Depending on molecular mass the thickness of an adsorbed polymer layer ranges from some twenty to one hundred nanometers [8]. In the adsorbed layer the polymer segment density is increasing with decreasing distance from the surface, so that the diffusion coefficient will be an involved function of distance. The experimental admittance data refer to a frequency range where the effective diffusion layer extends some 1000 nm. More detailed experiments will be necessary to find out whether this retardation effect quantitatively explains the observed increase of σ .

The differences between σ values for PVA vs PVP may provide some more insight in this retardation effect. With PVA the σ value is increased over the whole range of negative surface charges ($\text{pAg} > 4.5$ [8]). This could possibly be due to specific immobilization of iodide ions by PVA. It is known that iodine forms a complex with PVA, and that iodide ions are essential for this complex formation [28]. Probably iodide is responsible for forcing the polymer into a helix [29], leading to the coloured iodine-complex. The PVP-iodide complex is notably weaker than the PVA-iodide complex, as expressed by the marked dependence on molecular weight of the light absorption of $\text{I}_2 \cdot \text{I}^- \cdot \text{PVP}$ complexes [30].

5. Conclusions.

The results discussed above give rise to some general remarks and conclusions. Firstly, the electrostatics of the AgI/solution interface are fully described by its double layer capacitance and a diffusional impedance for the exchange of Ag^+ or I^- ions. This holds true for (i) solutions with various electrolyte concentrations; (ii) various interfacial potentials (Ag^+/I^- activities); (iii) an AgI surface covered with adsorbed polymer (or with EG present). Secondly, there is reasonable agreement between capacitance data from electrode impedance spectra and those obtained by other experimental techniques. This applies most clearly to data for plain electrolyte solutions, but similar trends are also found when organic material present. Thirdly, for plain KNO_3 solutions good agreement exists between our diffusion data and those presented in the literature. Comparison with values calculated from diffusion theory shows good agreement when silver ions are present in concentrations higher than 10^{-6} M, and less agreement when iodide is the

dominant ion. σ values have not yet been published for the silver iodide/solution interface in the presence of polymers, thus prohibiting any comparison.

In a forthcoming publication we will illustrate the relevance of the present results for the stability of AgI colloids. This discussion will focus on a comparison of time constants for several types of double layer relaxation processes at the AgI particle/solution interface, with the duration of particle interaction in the colloid as ensuing from Brownian motion [16].

6. References.

- 1 B.V.Derjaguin and L.Landau, *Acta Phisicochim. URSS*, **14** (1941), 633.
- 2 E.J.W.Verwey and J.Th.G.Overbeek, "Theory of the Stability of Lyophobic Colloids", Elsevier Publishing Co., New York, 1948.
- 3 B.H.Bijsterbosch and J.Lyklema, *Adv. Colloid Interface Sci.* **9** (1978), 127.
- 4 K.J.Peverelli and H.P.van Leeuwen, *J. Electroanal. Chem.*, **99** (1979), 151.
- 5 G.A.Finch, in G.A.Finch (ed.), "Polyvinylalcohol", Wiley, 1973, Section 19; and B.H.Carroll, *Photogr. Sci. Eng.*, **21** (1977), 151.
- 6 J.N.de Wit, Ph.D. thesis, Wageningen, 1975; J.N.de Wit and J.Lyklema, *J. Electroanal. Chem.* **41** (1973), 259.
- 7 B.Vincent, B.H.Bijsterbosch and J.Lyklema, *J. Colloid Interface Sci.*, **37** (1971), 171.
- 8 L.K.Koopal, Ph.D. thesis, Wageningen, 1978; L.K.Koopal and J.Lyklema, *Far. Discuss. Chem. Soc.*, **59** (1975), 230.
- 9 H.A.van der Schee, Ph.D. thesis, Wageningen, 1984.
- 10 K.J.Peverelli and H.P.van Leeuwen, *J. Electroanal. Chem.*, **110** (1980), 119.
- 11 K.J.Peverelli and H.P.van Leeuwen, *J. Electroanal. Chem.*, **110** (1980), 137.
- 12 K. Kvastek and V. Horvat, *J. Electroanal. Chem.* **130** (1981), 67.
- 13 K. Kvastek and V. Horvat, *J. Electroanal. Chem.* **147** (1983), 83.
- 14 J.H.A. Pieper and D.A. de Voys, *J. Electroanal. Chem.*, **53** (1974), 243.
- 15 R.B. Polder, B.H. Bijsterbosch and H.P. van Leeuwen, *J. Electroanal. Chem.*, **170** (1984), 175.
- 16 R.B. Polder, Ph.D. thesis, Wageningen, 1984.
- 17 D.J.C. Engel, Ph.D. thesis, Utrecht, 1968.
- 18 B.J.R. Scholtens, Ph.D. thesis, Wageningen, 1977.
- 19 G.J. Fleer and J. Lyklema, in "Adsorption from Solution at the Solid/Liquid Interface", G.D. Parfitt and C.H. Rochester (eds.), Academic Press, London etc, 1983, p.153.
- 20 H.P. van Leeuwen, in A.J. Bard (ed.), "Electroanalytical Chemistry", Vol. 12, Marcel Dekker, New York, 1982, p.159.

- 21 M. Sluyters-Rehbach and J.H. Sluyters in A.J. Bard (ed.), "Electroanalytical Chemistry", Vol. 4, Marcel Dekker, New York, 1970, p.1.
- 22 B. Timmer, M. Sluyters-Rehbach and J.H. Sluyters, J. Electroanal. Chem. 15 (1967), 343.
- 23 J.H.A. Pieper, D.A. de Vooy and J.Th.G. Overbeek, J. Electroanal. Chem. 65 (1975), 429.
- 24 J. Lyklema, Croat. Chim. Acta, 42 (1970), 151.
- 25 J. Lyklema, Kolloid-Z. 175 (1961), 129.
- 26 J. Lyklema and J.N. de Wit, J. Electroanal. Chem. 65 (1975), 443.
- 27 K.J. Peverelli, unpublished results.
- 28 G.J. Fleer, Ph.D. thesis, Wageningen, 1971.
- 29 G.A. Finch in G.A. Finch, (ed.), "Polyvinylalcohol", Wiley, 1973, p. 505.
- 30 M.A. Cohen Stuart, private communication.

Chapter V.

ELECTRODYNAMICS OF THE AgI/SOLUTION INTERFACE
AND THE MEANING FOR COLLOID STABILITY.

1. Introduction.

The DLVO theory [1,2] of colloid stability has had great impact on the development of colloid science. Its introduction has opened large fields of investigation, and it has been established as a powerful tool in solving many fundamental and practical problems.

One of the main problems that has remained unsolved, however, concerns the question whether the double layers of the particles in a colloidal solution interact under equilibrium conditions or not. Alternatively the question is whether collision takes place under conditions of constant surface potential, i.e. fully relaxed double layer, or under conditions of constant charge. The two cases are schematically illustrated in Fig.1. The former requires adjustment of the surface charge during the finite time of interaction of two particles. The latter

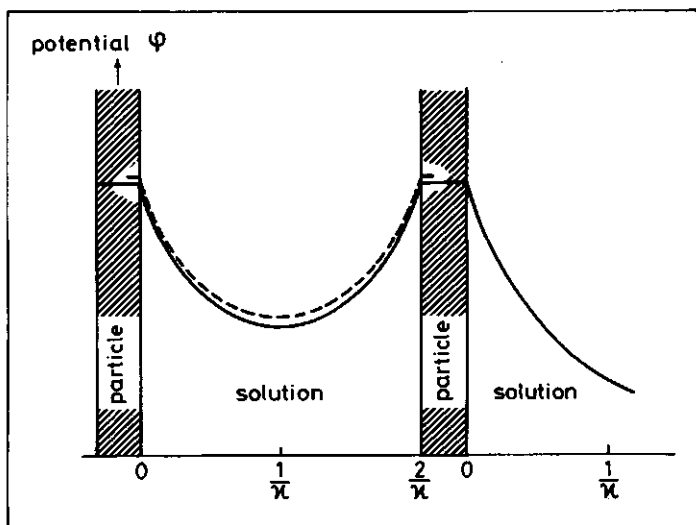


Fig.1. The profile of the double layer potential for a given value of the interparticle spacing. (—) constant surface potential, (----) constant charge density.

applies if the surface charge cannot adjust itself to the increase of the potential that results from the overlap of the electrical double layers during the collision.

Experiments on suspensions cannot be used to solve this question. The definition of the coagulation concentration and its experimental determination are not refined enough to clarify the matter. Titration measurements are basically unsuitable since they are performed under equilibrium conditions. To answer the question of 'constant potential' or 'constant charge', experiments have to be carried out that attack the problem directly. It is here that dynamic investigations, e.g., on electrodes consisting of the material under study, come into the picture. When an electrode surface that is in contact with a solution of such composition that it resembles the coagulation conditions of the corresponding colloid, is forced away from the equilibrium potential, some of the processes that possibly restore equilibrium can be studied in a direct manner.

Many investigations referred to above have been carried out on silver iodide as a model substance, because of the reproducibility in the preparation of suspensions and electrodes of this material [3]. Its colloidal and electrochemical properties are well-established. Since the sixties a lot of studies have been carried out on electrodes of silver iodide [4,5,6]. More recently, Peverelli and Van Leeuwen [7] and Kvastek and Horvat [8] have broadened the scope by not only considering the double layer capacitance, but also the ion transfer dynamics. The present study is an elaboration on this work, and it resulted in the total elucidation of the impedance and its components [9]. In contrast with earlier analyses, it appears that the rate of exchange of Ag^+ or I^- ions between AgI and the solution is determined by the transport in solution, rather than by the actual transfer step. Data on relaxation of AgI electrodes covered with an adsorbed layer of polymer molecules also provides new information [10].

In a paper on the possible relaxation processes during colloidal interaction, Lyklema [11] arrives at the conclusion that conditions of constant charge prevail. His work is based on theoretical considerations, and on the experimental evidence [7] that the Stern layer does not relax via exchange of ions between the solution and the AgI . Lyklema leaves open the bypasses of short-circuiting of the Stern layer via the

diffuse part of the double layer in solution, and relaxation by fast silver ion conduction through the solid. In a subsequent article by Lyklema and Van Leeuwen [12], this latter issue was worked out. It was assumed that ion transfer through the interface at the interaction area is slow, but that relaxation in the diffuse layer in solution and in the solid (involving conduction via interstitial silver ions) is fast. The authors conclude that this double diffuse double layer adjustment allows the potential at the region of interaction to relax during the collision. The 'excess' charge is smeared out over that part of the surface that is not in interaction with another particle. In Fig.2. we have schematically pictured this process.

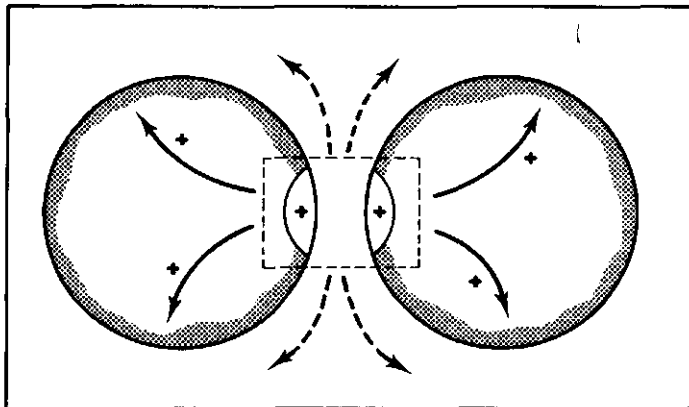


Fig.2. Schematic representation of two particles in collision. The indicated area is the interaction region; the shaded area depicts the region not directly involved in the interaction. The solid arrows indicate the flux of interstitial silver ions, dashed arrows indicate the relaxation of the diffuse layer in solution.

It is the purpose of the present paper to reconsider the issue on the basis of the new electrodynamic information [10]. Especially since it has been established that ion transfer across the interface is a rapid process, the picture has to be modified by putting more emphasis on diffusional mass transport of Ag^+ and I^- in solution.

2. Electrostatics of the AgI/solution interface: available information.

The experimental data has been obtained by analysis of the impedance spectrum of silver iodide electrodes [9]. The preparation of the electrodes and the experimental setup have been described elsewhere [13]. It was shown [9], that for periods longer than 10^{-6} s the impedance is fully described by a parallel arrangement of a double layer capacitance C and a diffusional (mass transport) impedance Z_W , as pictured in Fig.3.

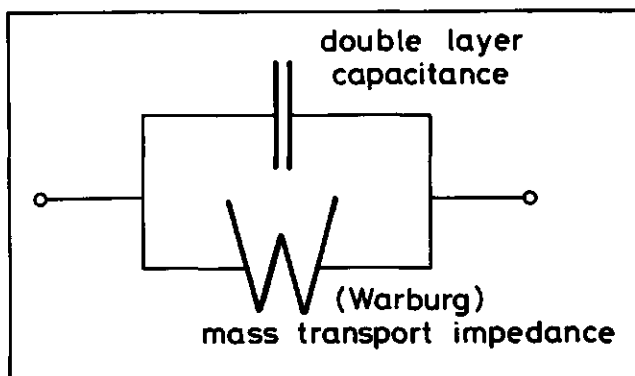


Fig.3. Electrical equivalent circuit of the AgI/solution interface.

The double layer capacitance includes adsorption of Ag^+ or I^- . Since the experimental conditions resemble coagulation conditions of colloids (0.1 M KNO_3 solution), the large excess of inert electrolyte makes $t_{Ag^+} = t_{I^-} \sim 0$, and the transport of Ag^+ and I^- ions in solution may be considered mass transport. In the case of semi-infinite linear diffusion, the transport impedance Z_W is given by [14]:

$$Z_W = Z' - j Z'' = (1-j) \sigma \omega^{-\frac{1}{2}} \quad (1)$$

where Z is the complex impedance, Z' its real and Z'' its imaginary component, $j = \sqrt{-1}$, σ is the Warburg coefficient and ω the angular frequency in $rad\ s^{-1}$. The Warburg coefficient is related to the concentration c_1 and the diffusion coefficient D_1 of the diffusing ion:

$$\sigma = R T F^{-2} c_1^{-1} (2 D_1)^{-\frac{1}{2}} \quad (2)$$

with R, T and F having the usual meaning. Experimental results [10] agree with the Warburg coefficients predicted from eqn(2), except for $pAg > 10$, where the experimental σ values are somewhat larger than the theoretical ones.

Our capacitance results agree with literature data obtained by titration of AgI suspensions [15], for plain 0.1 M KNO_3 solutions as well as when polymer was adsorbed on the electrodes. Similar agreement with literature data was found for the diffusion impedance in plain electrolyte solutions [7,8]. (Prior to [10], no data had been published on diffusion properties of this system in the presence of adsorbed polymer.)

The influence of the polymers poly (vinylpyrrolidone) (PVP, $M \sim 9 * 10^5$) and poly (vinylalcohol) (PVA, $M \sim 9 * 10^4$) was mainly to decrease the capacitance over a wide potential range, and to increase the Warburg coefficient for potentials more negative than corresponding with pAg about 8.

pAg	no polymer			PVP ($M \sim 9 * 10^5$)			PVA ($M \sim 9 * 10^4$)		
	σ	C	τ_w	σ	C	τ_w	σ	C	τ_w
4	600	50	2	600	50	2	600	40	1.2
6	9000	14	33	9000	10	17	15000	10	47
10	13000	10	35	18000	8	43	20000	7.5	47
12	3500	10	2	6000	8	5	9000	6	6
13	1500	19	2	3000	12	3	6000	7	4

Table I. Experimental relaxation parameters. Electrolyte 0.1 M KNO_3 .
 $T = 25^\circ C$. σ in $\Omega cm^2 s^{-\frac{1}{2}}$, C in $\mu F cm^{-2}$ and τ_w in msec.

In Table I we have collected the capacitances C and the Warburg coefficients σ for a number of pAg values, for 0.1 M KNO_3 solutions without polymer as well as with PVP or PVA adsorbed onto the electrodes.

Also shown is the relaxation time for semi-infinite linear diffusion, τ_W , as defined by [16]:

$$\tau_W = 2 \sigma^2 C^2 \tag{3}$$

Its physical significance is visualized by considering the time dependence of the overpotential η in the case of an infinitely short charge injection (and diffusion controlled relaxation), as it is given by [16]:

$$\eta(t) = \eta_0 \exp(t/\tau_W) \operatorname{erfc}(t/\tau_W)^{\frac{1}{2}} \tag{4}$$

Here η_0 is the initial overpotential and erfc is the error function complement. For $t = 0.69 \tau_W$ the overpotential is half its initial value. As compared to a purely exponential function, eqn(4) shows a rapid decay at short intervals, and a slow decay in the later part of the curve. This is schematically pictured in Fig.4. For more details the reader is referred to the electrochemical literature [16,17].

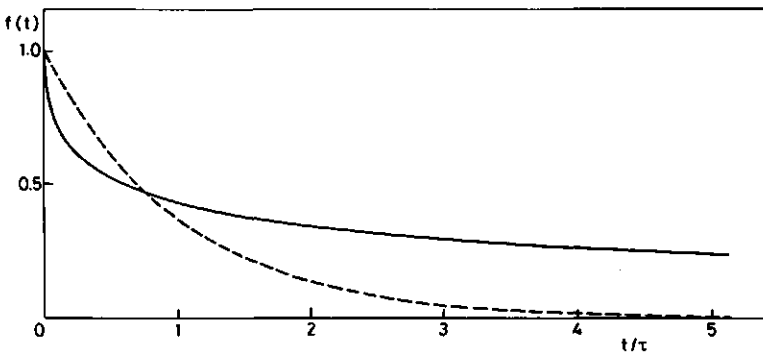


Fig.4. The functions $\exp(x)$ (broken curve) and $\exp(x)\operatorname{erfc}(x)$ (solid curve) vs time.

The relaxation time for ion transfer across the interface is given by:

$$\tau_{tr} = \theta C \tag{5}$$

with θ being the ion (charge) transfer resistance and C the interfacial capacitance. The relaxation of the overpotential for this case

(controlled by some activation process) will display an exponential course. A finite charge transfer resistance would show up as an incline of the curves in the real admittance plots, as discussed in ref [9]. In a previous paper [10] it has been shown, however, that these plots are horizontal for all potentials and also in the presence of adsorbed polymer. Particularly the absence of a detectable charge transfer resistance for the highest concentrations of silver or iodide ions, where τ_w is small, points towards a high rate of interfacial ion exchange. From the admittance plots it can be deduced that the upper limit of the ion transfer resistance is $5 \Omega \text{ cm}^2$.

3. Time scales of interaction and relaxation processes.

3.1. particle interaction.

The time of interaction of two spherical colloidal particles in the collision process, that is pictured in Fig.2, has been estimated by Lyklema. The simplest approach, based on Brownian motion, leads to [11]:

$$\tau_{Br} = (2 \kappa^{-1})^2 / 2 D_p = (12 \pi \eta a) / (\kappa^2 k T) \quad (6)$$

with D_p the diffusion coefficient of the particles, a their radius, κ the reciprocal Debye length, η the viscosity, k the Boltzmann constant and T the temperature. If a ranges between 100 and 500 nm, $\kappa \sim 10^{-9} \text{ m}^{-1}$ (0.1 M 1-1 electrolyte) and the other quantities have their usual values, eqn(6) yields values for τ_{Br} around 10^{-5} s .

Hydrodynamic effects will slow down the motion of the particles. Honig et al. [18] have evaluated the drag factor as about 10, depending on distance and particle radius. The corrected Brownian interaction time τ_{Br} thus becomes about 10^{-4} sec .

The geometry of the interaction area between the particles requires some special attention. The projection of two particles, their double layers and the various distances are pictured in Fig.5. If overlap is taken as the interparticle distance being smaller than $2\kappa^{-1}$, it can easily be shown from this picture that the region of overlap between the two double layers is a lens-shaped volume with the largest radius being equal to $(2a/\kappa)^{\frac{1}{2}}$. In calculations in the following sections the distance $(2a/\kappa)^{\frac{1}{2}}$ will be used as the characteristic length of the disequilibrated part of the double layer and the particle surface.

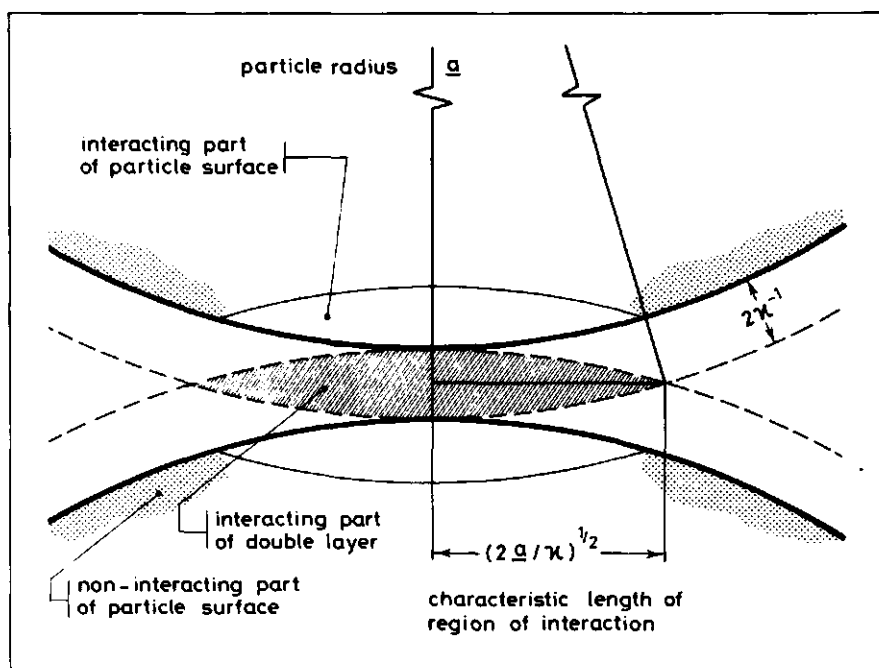


Fig.5. Schematic picture of two interacting spherical colloidal particles, with the emphasis on geometry. a is the particle radius, κ^{-1} the Debye length. The shaded area is the interaction region.

The various routes along which the disequibrated double layer in the colloidal system may relax are illustrated in Fig.6. The indicated processes are: I interfacial transfer of exchangeable ions, i.e. Ag^+ and I^- ; II diffusion into solution of Ag^+ or I^- ; III relaxation of the diffuse double layers at the two sides of the interface, in the solid by migration of interstitial silver ions; IV surface relaxation via diffusion and/or conduction of Stern ions. They will be subsequently dealt with in the following sections. An electrical equivalent circuit of a particle in interaction is given in Fig.7. A^* and C^* denote the disequibrated part of the surface and capacitance respectively. θ is the ion transfer resistance (process I in Fig.6). R_{AgI} denotes the resistance of the route along which the excess charge accumulated in C^* may leak away by interstitial silver migration (process III in Fig.6). Z_s denotes the relaxation of the excess charge by surface diffusion/

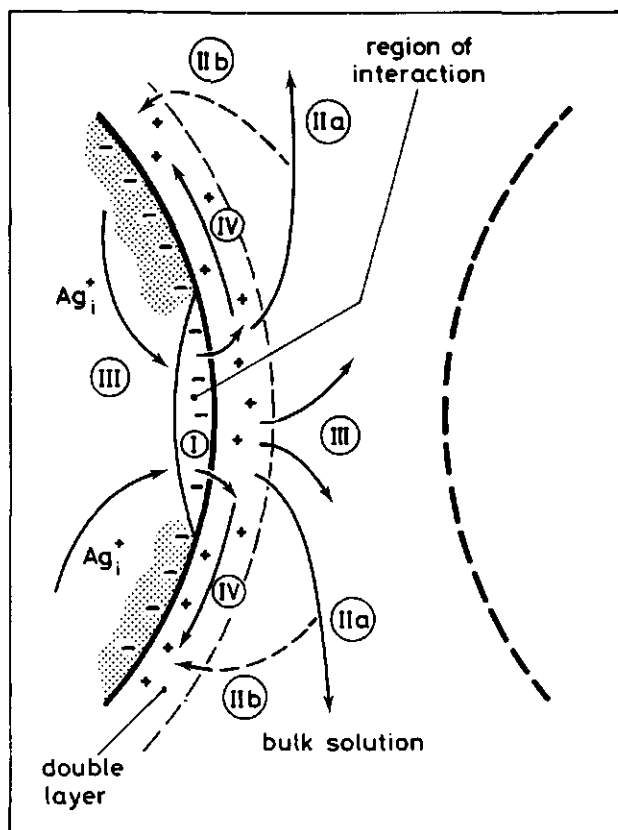


Fig.6. Possible relaxation routes for the surface charge, I interfacial ion transfer, II diffusion in solution, III relaxation of the diffuse layers, IV surface migration.

conductance (IV in Fig 6). Z_w denotes diffusion in solution (and resorption) as the equilibrating process (II). A^0 and C^0 denote that part of the surface and the capacitance which are not directly involved in the interaction.

3.2.interfacial ion transfer.

The mechanism by which the local excess charge on the particle ensuing from a collision may be transferred from the solid to the solution, is interfacial ion transfer. In Fig.6 this process is

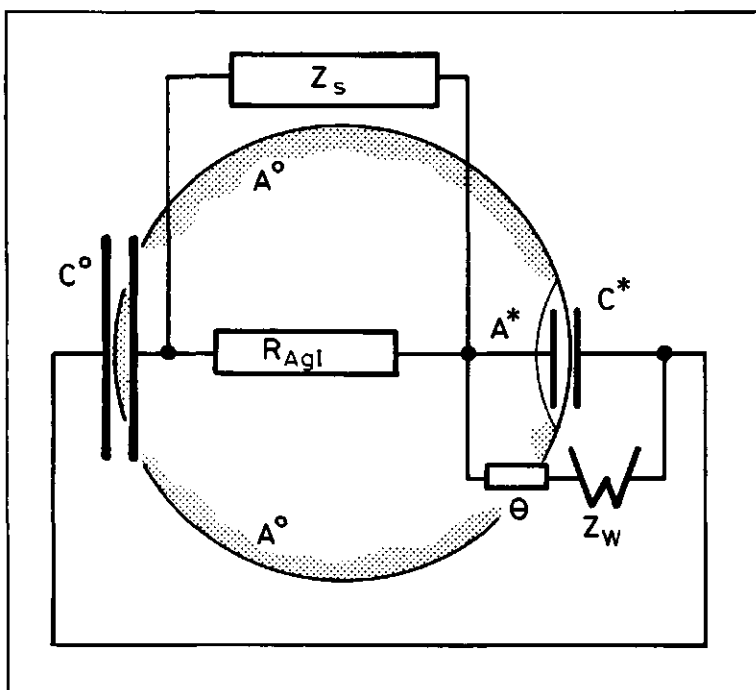


Fig.7. The electrical equivalent circuit of a colloidal particle in interaction. A^* and C^* denote the disequibrated fraction of the surface, A° and C° the remainder part. θ stands for ion transfer (corresponds with I in Fig.6); Z_W is the diffusion impedance (II in Fig.6); Z_s the surface relaxation impedance (IV in Fig.6), and R_{AgI} the bulk silver iodide conductance (III in Fig.6).

indicated as I. For negative particles this requires transfer of iodide ions from the AgI lattice to the solution side. These iodide ions can be further removed from the region of double layer overlap by one of the processes described in the following sections. For positively charged particles silver ions have to desorb (silver ion transfer being the crucial factor).

As mentioned in section 2, our experimental data on AgI electrodes indicate fast ion transfer. Under the conditions usually pertained to stability studies (pAg 12) $C \sim 10 \mu\text{F cm}^{-2}$, so with $\theta < 5 \Omega \text{ cm}^2$ and eqn(5) we obtain typically $t_{tr} < 5 * 10^{-5}$ sec. It is concluded that ion transfer is at least as fast as a Brownian collision, and in the equivalent circuit the component θ may be neglected.

3.3. diffusion in solution.

Once the excess ions have been desorbed, they have to be removed from the 'region of interaction'. One possible pathway of transport is diffusion into the solution, in Fig.6 designated by II^a. For linear diffusion from the interface an estimate of the relaxation time is given by eqn(3). In principle this equation applies to planar geometry. The thickness of a diffusion layer developed on the time scale of τ_{Br} , however, would be thicker by orders of magnitude than the particle separation. As the discussion on relaxation times only concerns orders of magnitude, we will omit the cumbersome rigorous evaluation of τ_w for the much more complex geometry of the colloid situation. We can, however, improve the estimate of eqn(3) using some additional considerations. As is illustrated in Fig.8, the overall diffusion process contains elements of planar diffusion (8.a) and spherical diffusion (8.b). For a given concentration gradient ΔC the flux equation would have a form like [19]:

$$\Phi = D \Delta C [(\pi D t)^{-\frac{1}{2}} + 1 / r] \quad (7)$$

with D the diffusion coefficient of the ions, t the time and r the radius of the 'sphere'. The term $(\pi D t)^{\frac{1}{2}}$ stands for planar diffusion, the 1/r term for spherical diffusion. In colloidal reality the combination of the two terms would be a cumbersome task. Let it suffice here to compare the relative weights of planar and spherical terms. On the time scale of particle interaction, as we have seen, t is of the order of 10^{-4} sec. With $D = 2 * 10^{-5} \text{ cm}^2 \text{ sec}^{-1}$, the first term will be ca. 10^{-3} nm^{-1} . If for r the characteristic length of the interaction region, $(2a/k)^{\frac{1}{2}}$ being ca. 50 nm, is taken, then the 1/r term is $2 * 10^{-2} \text{ nm}^{-1}$, so spherical diffusion is dominant and the flux thus is at least ten times larger than for planar diffusion only. Of course, this is still a crude approximation. The geometry is much more complex than purely spherical and the two particles act as obstacles, partly blocking diffusion. On the other hand, resorption of the excess Ag^+ or I^- onto a non-excited part of the particles (process II^b in Fig.6) will occur. Since ion transfer is fast, an iodide ion diffusing away from the region of interaction, A^* , may be incorporated in the lattice somewhere else on

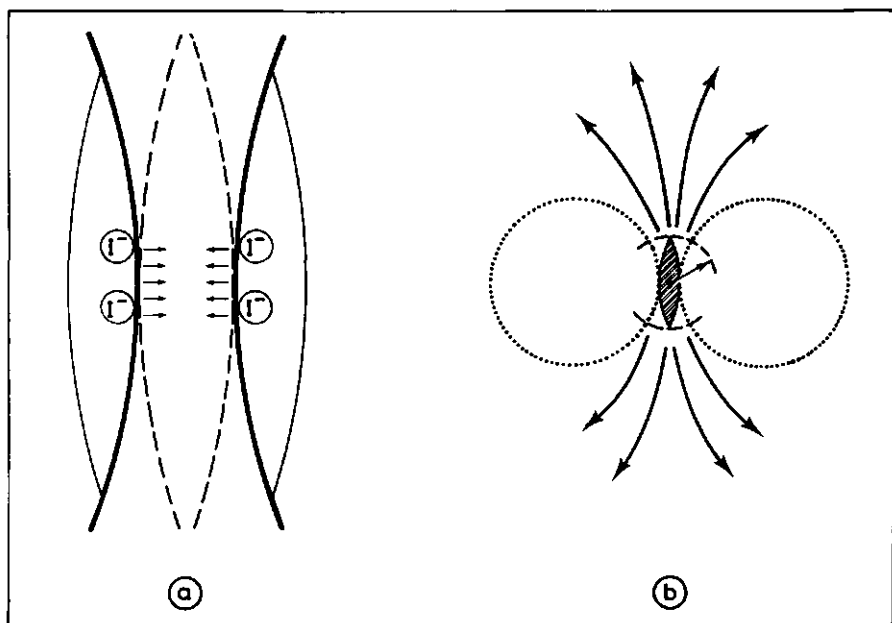


Fig.8. Schematical illustration of the diffusion process: a. planar diffusion for very small distances from the surface; b. spherical-like diffusion for larger distances. The radius of the "diffusion sphere" is on the order of $(2a/\kappa)^{1/2}$. For the sake of clarity, the particles are drawn relatively small as compared to the double layer thickness.

the surface of the particle, on A^0 . The reason for this phenomenon is that the local iodide concentration is in excess of the equilibrium concentration corresponding with the surface charge on A^0 . Of course, locally the potential is increased by this resorption, but as $A^0 \gg A^*$, the increase will be small. This resorption will increase the concentration gradient in solution, thus accelerating diffusional relaxation.

Another important aspect is the enhancement of transport by convection as caused by solution flows around the particles.

We conclude that eqn(3) overestimates the relaxation time for this system. Depending on the value of the equilibrium potential it yields: $10^{-3} < \tau_w < 5 \cdot 10^{-2}$ sec, as shown in Table I, also in the presence of adsorbed polymer. Taking into account the modification of the diffusion by sphericity effects, the relaxation times are reduced by a factor of

about ten, thus yielding ca. 10^{-4} sec. Considering the qualitative importance of other effects like resorption and convection, it seems quite likely that the relaxation is still considerably faster. It may be concluded, therefore, that at least partial relaxation via this route can take place.

3.4. relaxation of the diffuse layers.

Simultaneous relaxation of the space charge layer in the solid phase and the diffuse double layer in solution has been treated by Lyklema and Van Leeuwen [12]. They used a as the characteristic distance, whereas we adopted $(2a/\kappa)^{1/2}$. In Fig.6 this process is indicated by III. The relaxation time τ_d can be estimated from

$$\tau_d \sim (\rho_{AgI} + \rho_{soln}) * C_{interface} * (2a/\kappa)^{1/2} \quad (8)$$

With $\rho_{AgI} \sim 10^4 \Omega \text{ cm}$, $\rho_{soln} \sim 60 \Omega \text{ cm}$, $C_{interface} \sim 10 \mu\text{F cm}^{-2}$, and $(2a/\kappa)^{1/2} \sim 50 \text{ nm}$, we find $\tau_d < 5 * 10^{-7} \text{ sec}$.

Relaxation in the solid is the rate limiting process, but even this excess charge relaxation via migration of Ag^+ interstitials through the bulk of solid AgI is fast as compared to the time of interaction of colloidal particles. It is worth noticing that this process is substance dependent; if the conductivity would be much lower, this diffuse layer relaxation process might be slow as compared to the collision time.

3.5. surface relaxation.

There is another route to be considered for relaxation of the excess charge in the interaction region, namely processes along the particle surface, which we have indicated in Fig.6 as IV.

If the lateral relaxation via the Stern layer would proceed by diffusion, its relaxation time may be estimated from

$$\tau_s \sim (2a/\kappa) / 2 D_s \quad (9)$$

with $(2a/\kappa)$ as before and D_s the surface diffusion coefficient. As a first approach we take $D_s = D_{bulk}$, viz. $2 * 10^{-5} \text{ cm}^2 \text{ sec}^{-1}$ so that we have $\tau_s \sim 10^{-7} \text{ sec}$. This relaxation time may be longer, if the surface diffusion constant is lower than the bulk diffusion constant.

As the initial perturbation is a potential gradient along the surface, it seems likely that the surface relaxation has a predominantly conductive character, which will result in [11]:

$$\tau_s \sim (\epsilon \epsilon_0 / \kappa_s) (2a/\kappa)^{\frac{1}{2}} \quad (10)$$

where κ_s is the surface conductivity and $\epsilon \epsilon_0$ the local permittivity. We can substitute $\epsilon \sim 10$ (Stern layer!), $\epsilon_0 = 9 * 10^{-12} \text{ C V}^{-1} \text{ m}^{-1}$, and $\kappa_s \sim 10^{-8} \text{ } \Omega^{-1}$. The latter relatively high value, measured at pAg 12 by Van den Hoven for 0.1 M KNO_3 [20], results from a relatively high surface concentration of specifically adsorbed cations [21]. Now we have $\tau_s \sim 2 * 10^{-10} \text{ sec}$, which is faster than the estimate based on surface diffusion. The low dielectric constant makes the process ten times faster than in the bulk, all other parameters being equal. We conclude that lateral relaxation of the Stern layer is sufficiently fast to contribute to the relaxation of the double layer during particle interaction.

4. Conclusion.

All processes described in the previous sections have been shown to be either faster than or at least equally fast as the Brownian collision process. We have summarized the various processes and relaxation times in Table II. The conclusion may be drawn that the disequilibrated part of the double layer can adjust its charge to the dynamic circumstances in the colloidal solution. The surface charge of the remainder part of the particle may be temporarily increased by a negligibly small amount, that may relax on a longer timescale (via infinite diffusion into the bulk solution). **The interaction between particles in a silver iodide sol takes place under conditions of constant potential.** The influence of adsorbed polymers on the electrostatics of the system is small, and the large impact of adsorbed polymer on colloid stability must be attributed to, e.g., steric effects [22].

about ten, thus yielding ca. 10^{-4} sec. Considering the qualitative importance of other effects like resorption and convection, it seems quite likely that the relaxation is still considerably faster. It may be concluded, therefore, that at least partial relaxation via this route can take place.

3.4. relaxation of the diffuse layers.

Simultaneous relaxation of the space charge layer in the solid phase and the diffuse double layer in solution has been treated by Lyklema and Van Leeuwen [12]. They used a as the characteristic distance, whereas we adopted $(2a/\kappa)^{1/2}$. In Fig.6 this process is indicated by III. The relaxation time τ_d can be estimated from

$$\tau_d \sim (\rho_{AgI} + \rho_{soln}) * C_{interface} * (2a/\kappa)^{1/2} \quad (8)$$

With $\rho_{AgI} \sim 10^4 \Omega \text{ cm}$, $\rho_{soln} \sim 60 \Omega \text{ cm}$, $C_{interface} \sim 10 \mu\text{F cm}^{-2}$, and $(2a/\kappa)^{1/2} \sim 50 \text{ nm}$, we find $\tau_d < 5 * 10^{-7} \text{ sec}$.

Relaxation in the solid is the rate limiting process, but even this excess charge relaxation via migration of Ag^+ interstitials through the bulk of solid AgI is fast as compared to the time of interaction of colloidal particles. It is worth noticing that this process is substance dependent; if the conductivity would be much lower, this diffuse layer relaxation process might be slow as compared to the collision time.

3.5. surface relaxation.

There is another route to be considered for relaxation of the excess charge in the interaction region, namely processes along the particle surface, which we have indicated in Fig.6 as IV.

If the lateral relaxation via the Stern layer would proceed by diffusion, its relaxation time may be estimated from

$$\tau_s \sim (2a/\kappa) / 2 D_s \quad (9)$$

with $(2a/\kappa)$ as before and D_s the surface diffusion coefficient. As a first approach we take $D_s = D_{bulk}$, viz. $2 * 10^{-5} \text{ cm}^2 \text{ sec}^{-1}$ so that we have $\tau_s \sim 10^{-7} \text{ sec}$. This relaxation time may be longer, if the surface diffusion constant is lower than the bulk diffusion constant.

As the initial perturbation is a potential gradient along the surface, it seems likely that the surface relaxation has a predominantly conductive character, which will result in [11]:

$$\tau_s \sim (\epsilon \epsilon_0 / \kappa_s) (2a/\kappa)^{\frac{1}{2}} \quad (10)$$

where κ_s is the surface conductivity and $\epsilon \epsilon_0$ the local permittivity. We can substitute $\epsilon \sim 10$ (Stern layer!), $\epsilon_0 = 9 * 10^{-12} \text{ C V}^{-1} \text{ m}^{-1}$, and $\kappa_s \sim 10^{-8} \Omega^{-1}$. The latter relatively high value, measured at pAg 12 by Van den Hoven for 0.1 M KNO_3 [20], results from a relatively high surface concentration of specifically adsorbed cations [21]. Now we have $\tau_s \sim 2 * 10^{-10}$ sec, which is faster than the estimate based on surface diffusion. The low dielectric constant makes the process ten times faster than in the bulk, all other parameters being equal. We conclude that lateral relaxation of the Stern layer is sufficiently fast to contribute to the relaxation of the double layer during particle interaction.

4. Conclusion.

All processes described in the previous sections have been shown to be either faster than or at least equally fast as the Brownian collision process. We have summarized the various processes and relaxation times in Table II. The conclusion may be drawn that the disequilibrated part of the double layer can adjust its charge to the dynamic circumstances in the colloidal solution. The surface charge of the remainder part of the particle may be temporarily increased by a negligibly small amount, that may relax on a longer timescale (via infinite diffusion into the bulk solution). **The interaction between particles in a silver iodide sol takes place under conditions of constant potential.** The influence of adsorbed polymers on the electrostatics of the system is small, and the large impact of adsorbed polymer on colloid stability must be attributed to, e.g., steric effects [22].

relaxation process	symbol	magnitude/s
Brownian collision	τ_{Br}	10^{-4}
ion transfer	τ_{tr}	$< 5 * 10^{-5}$
Warburg diffusion corrected for sphericity	τ_W	10^{-3} to $5 * 10^{-2}$ 10^{-4}
diffuse double layer	τ_d	$5 * 10^{-7}$
surface conduction (, , diffusion	τ_s	$2 * 10^{-10}$ 10^{-7})

Table II. Relaxation processes and the orders of magnitude of the relaxation times.

5. References.

- 1 B.V.Derjaguin and L.Landau, *Acta Phisicochim. URSS*, **14** (1941), 633.
- 2 E.J.W.Verwey and J.Th.G.Overbeek, "Theory of the Stability of Lyophobic Colloids", Elsevier Publishing Co., New York, 1948.
- 3 B.H.Bijsterbosch and J.Lyklema, *Adv. Colloid Interface Sci.*, **9** (1978), 127.
- 4 J.J.C.Oomen, Ph.D. thesis, Utrecht, 1966.
- 5 D.J.C.Engel, Ph.D. thesis, Utrecht, 1968.
- 6 J.H.A.Pieper and D.A.de Vooy, *J.Electroanal.Chem.* **53** (1974), 243.
- 7 K.J.Peverelli and H.P.van Leeuwen, *J.Electroanal.Chem.*, **110** (1980), 119, 137.
- 8 K.Kvastek and V.Horvat, *J.Electroanal.Chem.*, **130** (1981), 67; **147** (1983), 83.
- 9 R.B.Polder, B.H.Bijsterbosch and H.P.van Leeuwen, *J.Electroanal.Chem.*, **170** (1984), 175.
- 10 R.B.Polder, B.H.Bijsterbosch and H.P.van Leeuwen, *J.Electroanal.Chem.*, submitted
- 11 J.Lyklema, *Pure Appl.Chem.*, **52** (1980), 1221.
- 12 J.Lyklema and H.P.Van Leeuwen, *Advances Colloid Interface Sci.* **16** (1982), 127.
- 13 R.B.Polder, Ph.D. thesis, Wageningen, 1984.
- 14 M.Sluyters-Rehbach and J.H.Sluyters in A.J.Bard, (Ed.), *Electroanalytical Chemistry*, Vol.4, Marcel Dekker, New York, 1970, p.1.
- 15 L.K.Koopal, Ph.D. thesis, Wageningen, 1978;
H.A.van der Schee, Ph.D. thesis, Wageningen, 1984;
J.N.de Wit, Ph.D. thesis, Wageningen, 1975.
- 16 W.H.Reinmuth, *Anal.Chem.*, **34** (1962), 1272.
- 17 H.P.van Leeuwen in A.J.Bard, (Ed.), *Electroanalytical Chemistry*, Vol.12, Marcel Dekker, New York, 1982, p.159.
- 18 E.P.Honig, G.J.Roeberson and P.H.Wiersema, *J.Coll.Interface Sci.*, **36** (1971), 97.
- 19 K.J.Vetter, *Elektrochemische Kinetik*, Springer-Verlag, Berlin, 1961.
- 20 T.J.J.van den Hoven, Ph.D. thesis, Wageningen, to be published.
- 21 J.N.de Wit and J.Lyklema, *J.Electroanal.Chem.*, **41** (1973), 259.
- 22 J.M.H.M.Scheutjens and G.J.Fleer, *Macromolecules*, submitted.

ABSTRACT.

The purpose of this study is to gain insight in electrodynamic processes in colloidal systems, that is, in the electrical currents that flow because of the movement of charged particles. There is a need for such insight, because the DLVO theory describing the stability of electrostatic colloids cannot answer the following question: can interacting particles in the short time of Brownian encounter adjust their charge to the disequilibrium resulting from the overlap of the double layers and thus keep their **potential constant**? Or will the particles keep their **charge constant** during the interaction? The answer depends on the rate of various possible charge transfer processes. We have chosen for electrodes to investigate the dynamic phenomena of interest, and for AgI as the model substance.

Chapter I offers a general introduction to the theme, and describes the outline of this study.

The experimental technique used (the coulostatic impulse method) is based on the following experiment. A small departure from the equilibrium potential is instantaneously imposed on two identical electrodes. The overpotential relaxes and the decay, of which the precise shape contains information on the various processes, is recorded. In **chapter II** we describe the preparation of the AgI electrodes and the other materials, the setup and the procedure to convert the decay signal into an impedance spectrum.

In **chapter III** an analysis of the impedance spectrum is made, and the possible components of the electrical equivalent circuit are discussed. It is shown that surface roughness of the electrode seriously complicates the mass transport impedance and this may ruin the analysis of the impedance spectrum. It is concluded that the combined analysis of two admittance functions, employing both the real and imaginary components, provides the best method: it allows to clearly recognize the effects of surface roughness, and the analysis can easily be automated. It is also shown that ion transfer through the interface is a rapid process, and that diffusion in the solution (mass transport) is the rate limiting step.

In **chapter IV** experimental results are presented in terms of capacitances and Warburg (diffusional) coefficients under various conditions of potential and electrolyte concentration. The data refer to 'clean' electrodes, as well as to electrodes with an adsorbed polymer layer. The polymers used were PVA (M ca. $9 * 10^4$) and PVP (M ca. $9 * 10^5$). The results are compared with literature data. Generally, the agreement was satisfactory, and a tentative explanation for the trends in the capacitances was forwarded. The Warburg coefficients showed some deviation from the theoretically expected behaviour, the more so when polymer was adsorbed.

Chapter V summarizes the literature on relaxation processes during interaction in colloids, and resumes the experimental information from the previous chapters. Particularly the assessment of ion transfer as a fast process calls for a reconsideration of the hitherto existing picture. Three possible relaxation routes (after ion transfer) of the excess charge on the particle are described and relaxation times for each are estimated. It is concluded that silver iodide particles, uncovered or covered with a polymer layer, can adjust their surface charge on the time scale of a collision by at least one of the transport processes described. **The interaction thus takes place under conditions of constant potential.**

DE ELEKTRODYNAMIKA VAN HET ZILVER-JODIDE OPLOSSINGSGRENSVLAK.

SAMENVATTING.

Een kolloid (spreek uit als: kol-loo-wied) is een verzameling van kleine deeltjes van één fase (stof), die verdeeld zijn in een samenhangende hoeveelheid van een andere fase. De praktische toepassingen van de kolloidchemie zijn waarschijnlijk net zo oud als de beschaving. Om maar iets te noemen: een zeepoplossing is een kolloidaal systeem, dat aggregaten van meerdere zeepmolekulen bevat in een oplossing van aparte zeepmolekulen in water; melk is een verdeling van vetdruppeltjes in een waterige oplossing; een fotografische film bevat kristallijne zilver bromide (of zilver jodide-bromide) deeltjes als lichtgevoelige kerntjes, verdeeld in een "bevroren" gelatine oplossing.

De ingewikkeldheid van deze drie voorbeelden verschilt: zeep maken kan heel eenvoudig; melk heeft na produktie door de koe maar weinig aandacht nodig; een filmpje vereist een heleboel wetenschappelijke inbreng vóórdat men er ook maar de vaagste foto mee kan maken.

Met de huidige stand van technologie steunen vele produktieprocessen zwaar op inzichten in fundamentele processen achter kolloidale verschijnselen. Eén van die fundamentele processen is de stabiliteit van het kolloid. Blijven de deeltjes verdeeld of klonteren ze samen en 'vlokken ze uit'? Sinds de veertiger jaren bestaat er een theorie, de DLVO theorie, die de stabiliteit van kolloidale systemen als gevolg van hun lading met succes beschrijft. Ze kan echter niet de vraag beantwoorden: kunnen geladen kolloidale deeltjes hun lading aanpassen aan het elektrisch veld waarin ze tijdens botsingen met andere deeltjes tijdelijk verkeren? Is dit wel mogelijk, dan noemen we dat het geval van **konstante potentiaal**; zoniet, dan heet het **konstante lading**.

Het antwoord op deze vraag hangt af van de snelheid van de verschillende processen waardoor het deeltje lading kan uitwisselen met de oplossing. Wij hebben gekozen voor elektroden om de dynamische verschijnselen te onderzoeken, en voor zilver-jodide als modelstof.

Hoofdstuk I geeft een algemene inleiding en de opzet van dit proefschrift.

De gebruikte techniek, de coulostatistische puls methode, werkt als volgt. Twee identieke elektroden worden momentaan een beetje uit hun evenwichtspotentiaal gebracht. Daarna relaxeert de overpotentiaal, en de precieze vorm van de kurve die informatie bevat over de te onderzoeken processen, wordt opgenomen. **Hoofdstuk II** beschrijft de bereiding van de AgI elektroden, en de overige materialen, de opstelling en de methode waarmee de relaxatie-kurve omgezet wordt in een impedantie-spektrum.

In **Hoofdstuk III** wordt het impedantie-spektrum geanalyseerd, en de mogelijke onderdelen van het elektrische equivalent circuit besproken. Oppervlakte ruwheid blijkt de massa transport impedantie te compliceren, wat de analyse van het impedantie-spektrum sterk kan bemoeilijken. Het beste voldoet een gekombineerde analyse van het reële en imaginaire deel van de admittantie: zo kan men oppervlakte-ruwheid gemakkelijk herkennen, en de analyse kan eenvoudig geautomatiseerd worden. Het blijkt dat de overdracht van Ag^+ en I^- ionen door het grensvlak snel is, en dat diffusie in de oplossing (massa transport) snelheidsbeperkend is. In **Hoofdstuk IV** worden de experimentele resultaten weergegeven in termen van capaciteiten en Warburg (diffusie-impedantie) coëfficiënten bij verschillende potentialen en elektrolytconcentraties. De resultaten zijn verkregen met 'schone' elektroden, en die waar een polymeerlaag op geadsorbeerd was. De gebruikte polymeren waren PVA (M ca. $9 \cdot 10^4$) en PVP (M ca. $9 \cdot 10^5$). De resultaten worden vergeleken met de literatuur. In het algemeen komen ze goed overeen, en er wordt een poging gedaan het verloop van de capaciteit te verklaren. De Warburg coefficient vertoont lichte afwijkingen van het theoretisch verwachte gedrag, en des te meer met geadsorbeerd polymeer.

Hoofdstuk V geeft de literatuur over relaxatieverschijnselen bij interactie in kolloidale systemen kort weer, en vat de experimentele resultaten van de vorige hoofdstukken samen. Vooral de vaststelling dat ionenoverdracht snel is, noopt tot heroverweging van het bestaande beeld. Drie mogelijke routes worden beschreven, waarlangs de 'extra' lading op het deeltje kan wegvloeien, en de bijbehorende relaxatietijden worden geschat. De konklusie luidt, dat zilverjodide deeltjes, met of zonder geadsorbeerd polymeer, hun oppervlaktelading kunnen aanpassen tijdens de botsing door tenminste één van deze processen. De interactie in een zilverjodide sol vindt dus plaats met konstante potentiaal.

CURRICULUM VITAE.

Ik ben geboren op 13 maart 1952 in Den Haag. De lagere school bezocht ik te Rijswijk en Emmen. Van 1964 tot 1970 volgde ik een gymnasium- β opleiding aan de Rijksscholengemeenschap Wagenings Lyceum te Wageningen. In 1970 ging ik aan de Rijksuniversiteit Utrecht scheikunde studeren.

Mijn kandidaatsexamen S1 (scheikunde met wiskunde, natuurkunde en biologie) haalde ik in 1974. Mijn hoofdvak was anorganische chemie, bij Prof. Dr. G.H.J. Broers, dat ik voor een deel volgde aan de Rijksuniversiteit Groningen. Daar deed ik ook een bijvak algemene en arbeids-economie. Het doktoraalexamen behaalde ik in 1978.

Van 1 september 1979 tot 1 september 1983 was ik wetenschappelijk medewerker aan de Landbouwhogeschool Wageningen, bij de vakgroep Fysische en Kolloïdchemie, waar ik het in dit boekje beschreven onderzoek heb uitgevoerd.

Inmiddels ben ik benoemd tot wetenschappelijk medewerker bij het Instituut voor Bouwmaterialen en Bouwconstructies van TNO te Rijswijk.